UNIVERSIDADE DE LISBOA
FACULDADE DE CIÊNCIAS
DEPARTAMENTO DE FÍSICA

Optimizing miniature electrodes and current approaches to EEG analysis

Iara de Almeida Ivo

MESTRADO INTEGRADO EM ENGENHARIA BIOMÉDICA E BIOFÍSICA
Perfil em Engenharia Clínica e Instrumentação Médica

Dissertação orientada por:
Prof. Doutor Alexandre da Rocha Freire de Andrade
e co-orientado pelo Prof. Doutor Gunnar Waterstraat

2018

To my Sister.

You is kind. You is smart. You is important.

Aknowledgements

First of all, I'd like to thank the Erasmus+ program, for enabling one of the most valuable experiences I've had, personally and professionally.
A thank you to the institution, the faculty members and IBEB members, who all throughout the years led me in the right direction to be who I want to be as a professional.
Special thanks are in order to my internal supervisor, Professor Alexandre Andrade, not only for his guidance and feedback throughout this project but whose classes pushed me into a scientific field that passions me everyday and brings me joy.

A thank you to the Neurophysics group at the Charité Hospital in Berlin, who welcomed me with open arms into a professional environment like no other.
To Dr. Gabriel Curio and Dr. Vadim Nikulin, for taking me on as a pupil, for their ever so insightfull and knowleagable advices, for their patience and for their guidance throughout this process.
But especially to my external supervisor. My mentor. My friend. Gunnar Waterstraat. Who took me on, even though he was not meant to. Who taught me everything he could and more. From coding skills to life skills, from mathematical algorithms to patient care, passing by the dilemmas of scientific research. This work was only a glimpse into his world, teaching me to search for all the answers, to be the best one possibly can. I can only hope to be as brilliant of a professional one day.

Thank you to my family and friends, who supported me in this long journey, from a long distance, and that endured this time spent apart as if none had.
A special mention to Filipe Costa, Francisco Fernandes, Inês Veríssimo, Isabel Barradas and Joana Boita, who were there every step of the way, through every setback and every win. These are either people who make even the darkest days seem bright or that remind you of how much one can find peace in the dark. I would never have made it this far without them.
Thank you to my mother, who taught me early on that even the smallest girl can fight and achieve the biggest dreams.

And lastly, to my sister, who inspires me by her sheer existence. This work is as mine as is yours, I hope it inspires you in return.

Abstract

Many neurodegenerative and neuronal diseases use EEG as a primary diagnosis tool, providing reliable noninvasive real-time evaluation of neuronal processes in the human brain. For epilepsy patients, for example, monitoring the disorder will allow ascertaining if a seldom or rare occurring seizure corroborates a diagnosis or when investigating how many seizures happen during a day and locate them in space to reach a precise diagnostic plan. However a long EEG recording is still unideal for users. Day-long EEG's involve a bulky, eye-catching medical cap that provokes discomfort after a couple of hours as well as an undesirable appearence to the wearer. The EEG analysis technique has also been facing novel improvements over the last few decades such as the development sophisticated artifact detection and removal algorithms and improved head models for source estimation. Increasing the wearability of an EEG setup that also elevates the quality of signal using such novel techniques seems to be an important step towards other uses in the research (i.e. Brain Computer Interface applications) and medical communities.

The miniaturization of the EEG: both in size and weight but also visual perception, seems to be a logical step to elevate such a system. The idea that one could have smaller, miniaturized electrodes, without any sort of cap; came from the team of Dr. Vadim Nikulin et al[1]. The idealised new electrode system would be a portable, reliable, reusable, invisible, new device able to allow accurate medical diagnosis. Another goal of this dissertation would also be the development of analysis algorithms for EEG applications and studies that accompanies the hardware development and provides the EEG research and medical community with valuable analysis tools. The Electrodes developed are composed of an Ag/AgCl ring with a copper wire and a plasticized cable for easy maneuvering. They demonstrate similar amplitude range signal and SNR as standardly used EEG electrodes.

A DFA analysis for High Frequency Oscillations is useful in order to identify common bursts across subjects but also to speculate that the brain could work at a criticality point of the frequency spectrum. SSD is a spatial filtering technique that proved to extract accurately the strongest sources of alpha and theta activity across subjects, thus improving their signal-to-noise ratio. In a visual study of perceptual memory, it provided the conclusion that alpha oscillations not only influence perceptual bias but also the variability in the model and that strong regional theta oscillations are correlated with less effective visual detection, potentially due to drowsiness. Moreover, it allowed an accurate inverse source modelling analysis with the Brainstorm software, pointing at the occipital cortex as the origin that alpha wave range; while aiming the origin for the theta range frequency for an area concordant with the posterior cingulate cortex, both of these appointed in literature as sources for visual perception [2] [3]. The PCO algorithm could recover both the source pattern of the coupled alpha source as well as the original relation between the phase of the source signal. However,without the SSD preprocessing, PCO is prone to overfitting. PCO hopes to be a valuable tool to increase the sensitivity of phase coupling analyses and to localize the sources of phase coupling. Although this dissertation presents an EEG system composed of

miniaturized EEG electrodes as well as several analysis tools, future work needs to be developed in order to confirm the effectiveness of this approach when used on medical patients such as epilepsy patients.

Keywords: Electroencephalography, Electrode Manufacture, Brain Criticality, Phase Coupling Optimization, Spatial Spectral Decomposition, Detrended Fluctuation Analysis

Resumo

Inúmeras são as condiões neurodegenerativas, bem como as doenças neuronais no geral, que utilizam a técnica da Electroencefalografia - também denominada pela comunidade científica bem como nesta tese de dissertação, como EEG - enquanto principal método de diagnóstico. Esta técnica prima por se apresentar como um método não invásivo que permite a avaliação em tempo real dos processos neuronais do cérebro humano. Tomando por exemplo o caso de um paciente afectado com epilepsia, é-nos também fácil de deduzir que monitorizar a condição é uma atividade extremamente relevante para o diagnóstico, já que este processo permite identificar e classificar crises epilépticas que de outra forma não seriam identificadas. No entanto um exame de EEG de longa duração implica que o seu utilizador use uma pitoresca touca de EEG durante o seu dia-a-dia, cujo mecanismo de pressão provoca algum desconforto. A análise de um EEG tem também sofrido mudanças nas últimas decadas, tal como o desenvolvimento de algoritmos de identificação de artefatos e a evolução de novas técnicas de estimação de fontes de corrente elétrica cerebral. Melhorar a forma como se realiza uma medição de EEG é então um importante passo a tomar de forma a tornar a experiência mais confortável para o seu utilizador, tanto em aplicações médicas como a acima descrita bem como para outras aplicações relevantes i.e. no uso da técnica de *Brain Computer Interface*. A miniaturização dos elétrodos, em tamanho e por conseguinte em peso, de forma a aumentar o conforto e bem-estar do utilizador parecem ser então o passo lógico a tomar na direção de um melhor sistema de medição de EEG. A solução deste problema foi pensada primeiramente pela equipa do Dr. Vadim Nikulin et al[1], um novo equipamento, sem touca: portátil, reutilizável, invisivel, capaz das mesmas funcionalidades que um sistema de medição de EEG convencional, eficaz no diagnóstico médico.

Partindo deste ponto, todos os passos da manufatura dos elétrodos foram reavaliados de forma minuciosa. Foram tidos em conta diversos materiais e ligas condutoras para a produção do anel do elétrodo, sendo os mais duradouros e fidedignos os aneis de Ag/AgCl e de Au, os quais foram testados comparativamente com elétrodos *standard* em papel humedecido com uma solução de NaCl. Relativamente ao cabo, e de forma a reduzir o tempo necessário ao *setup*, aumentar o rácio de elétrodos produzidos viáveis bem como tornar os elétrodos reutilizáveis foi introduzido um cabo plastificado, que poderá ser ocultado facilmente através da roupa do utilizador, sendo que a porção exposta remanescente pertence ao cabo de cobre, mais fino do que um fio de cabelo, aproximadamente invisÃvel a olho nú. Os tempos e processo de electrólise foram também reformulados, tendo em conta o mais recente state-of-the-art, sendo que a eletrólise passou a ser feita num ambiente mais controlado, com recurso a uma hotte química pertencente ao parceiro do hospital Charité, a CWW - *Charité Centrum Wissenschaftliche Werksttätten - Charité Center Scientific* . O método de ligação do anel ao fim de cobre foi também melhorado, recorrendo novamente à CWW, sendo que no lugar de uma soldagem com uma solda de bico fino, foi efectuada uma soldagem microscópica. Após esta última reforma no processo de fabrico, o rácio, supra mencionado, de eléctrodos úteis após produção aumentou significativamente, de um terço para quatro quintos, o que por sua vez permitiu concluir o processo de desenvolvimento dos elétrodos.

Os mini elétrodos detalhados nesta tese de dissertação, enquanto protótipo final, são compostos por um anel de *Ag/AgCl*, conetados a um fio de cobre que por sua vez pode ser conetado ao amplificador por um fio plastificado que lhe confere uma maior capacidade de manuseamento. Estes demonstram uma amplitude de sinal similar bem como um rácio **signal-to-noise** semelhante aos elétrodos convencionais utilizados num meio hospitalar. Foi possível ainda observar eventos de activação das ondas da gama de frequência alpha, relacionados com uma experiência simples de *finger twitching* através de estimulação do nervo mediano, tal como descrito pela metodologia desenvolvida por [4], com 3.147 Hz de frequência de estimulação.

A optimização deste novo tipo de elétrodo descrita nesta tese de dissertação, acompanhada por um segundo objetivo: o desenvolvimento de algoritmos de análise do sinal de EEG, de forma a disponibilizar novas ferramentas de análise à comunidade de investigação e posteriormente à comunidade médica. Diversas medições e paradigmas, conduzidos por membros do grupo de *Neurophysics* do Hospital *Charité Universitätsmedizin* em Berlim foram utilizados para este efeito. Para o estudo de criticalidade em oscilações de altas frequências, foram utilizados dados de uma experiência efectuada em 2016 [5] com recurso a um amplificador construído para o efeito. Dez sujeitos foram estimulados no nervo mediano a uma frequência de 4.3 Hz, tendo por frequência de amostragem 10 Hz. Comprovando que as medições podem ser representadas como correlacionadas no tempo (*Long Range Temporal Correlation* podemos inferir se esta atividade é processada de forma crítica no cérebro. Esta correlação temporal foi quantificada utilizando as técnicas *Detrended Fluctuation Analysis* e *Canonical Correlation Analysis*. Concluiu-se que a utilização da técnica *Detrended Fluctuation Analysis* em Oscilações de altas frequências é capaz de identificar picos de atividade comuns entre sujeitos que podem corresponder a atividade cerebral crítica, corroborando a teoria da criticalidade cerebral. Para o estudo da influência das gamas de frequência alpha e theta na percepção humana, foram utilizados dados de uma experiência conduzida pela *Berlin School of Mind and Brain* [6]. Foram apresentadas imagens de filtros de *Gabor* intermitentemente com imagens vazias i.e. sem conteúdo, fundindo-se com a sala, a sujeitos numa sala escura. Após cada trial o sujeito responde se viu ou não uma imagem bem como se tem certeza desta resposta. Foi dado feedback aos sujeitos, após cada *trial*, relativamente à correção das respostas. A técnica de filtro espacial *Spatial Spectral Decomposition* permitiu extrair corretamente as fontes de atividade alpha e theta entre sujeitos bem como evidenciar a possibilidade de: uma correlação positiva entre a atividade de ondas de frequência alpha e a memória perceptual; e uma anticorrelação entre as oscilações de frequências theta e a deteção visual. Por fim, foi implementado um algorítmo de análise da correlação de fase entre uma actividade *trigger* e o seu sinal correspondente, denominada de *Phase Coupling Optimization* com o software *Matlab*. Este foi testado com os mesmos modelos *forward head models* que os utilizados em [7], que exibem fontes de ativação da gama de frequências alpha coincidentes temporalmente com um trigger, misturadas com fontes de ativação da gama de frequências alpha randómicas ao longo do sinal. Este algoritmo permitiu recuperar tanto o padrão de acoplamento entre a fonte de oscilações alpha com a atividade alvo correspondente bem como com a distância de fase do sinal entre ambas. No entanto, tornou-se óbvia a necessidade de aplicação de um passo de pré processamento espacial (como a SSD), já que a técnica demonstrou uma tendência a sobre ajustar os dados (*overfitting* entre sujeitos).

Esta dissertação apresenta algumas formas de análise de dados de EEG bem como um novo sistema de recolha dos mesmos, composto por mini elétrodos. No futuro serão necessários estudos de forma a comprovar a eficácia dos eléctrodos desenvolvidos bem como do sistema em si, num grupo de pacientes, de forma a corroborar a capacidade de diagnóstico dos mesmos.

Palavras-chave: Electroencephalografia, Produção de Eléctrodos, Criticalidade Cerebral, *Phase Coupling Optimization*, *Spatial Spectral Decomposition*, *Detrended Fluctuation Analysis*

Contents

List of Abbreviations

CCA Canonical Correlation Analysis
CT Computerized Tomography
CVC Communication-through-coherence
cSPoC canonical Source Power Correlation analysis
CWW Charité Centrum Wissenschaftliche Werksttätten [CharitÃ© Center Scientific Workshops]
EEG Electroencephalography
ERP Event-Related Potentials
FFT Fast Fourier Transform
FT Fourier Transform
fMRI Functional Magnetic Resonance Imaging
ILAE International League Against Epilepsy
LORETA Low Resolution Brain Electromagnetic Tomography
LRTC Long Range Temporal Correlation
LSD Linear Spectral Density
MEG Magnetoencephalography
MI Modulation Index
MLV Mean Vector Length
MR Magnetic Resonance
MRI Magnetic Resonance Imaging
PCO Phase Coupling Optimization
RMS Root Mean Square
SSD Spatial Spectral Decomposition
SNR Signal to Noise Ratio
WROP weighted resolution optimization

List of Figures

Chapter 1

Introduction

The diagnostic value of Electroencephalography (EEG) is of the utmost importance in neurological diseases and disorders, since it provides a simple non-invasive view on the electrical activity in the brain. This means that, although not a new technology, EEG is still in the first line of diagnosis tools when the suspicion of possible neurological prognosis arises. With the continuous evolution of software and programming, achieving more elaborate and precise EEG medical data analysis is increasingly ameliorating both the specificity and sensitivity of medical diagnostics and medical research.

The general purpose of this project was, in line of medical diagnostic research and diagnostic improvement, to optimise EEG technology both in hardware, in terms of optimal wearing comfort while still maintaining superior signal quality, as well as in data analysis.

Since epilepsy is, roughly put, a neuronal electrical disorder and EEG measures electrical activity originating from the brain, it is only natural that being of great diagnostic value, major breakthroughs in EEG, will be of extensive importance for epilepsy. This is why epilepsy was chosen as a case study and leading application of EEG in this work.

A strong focus of the work was the development and testing of miniaturised EEG electrodes, which were a particular interest at the time of the study to the Charité Hospital in Berlin, where this dissertation thesis has been developed. The mini-electrodes, which had already had some spotlight in the last three years, required some refinement in order allow their production for the hospital itself, but also to the University of Freiburg, through the RADAR-CNS project, funded by the European Union funding line Horizon 2020.

Additionally, the Neurophysics group at the Charité Hospital is involved in applied EEG-based research such as the analysis of somatosensory and visual processing. A variety of state-of-the-art analyses were explored in the obtained data, such as long range temporal correlations (LRTC), inverse source modeling and the analysis of somatosensory high-frequency oscillations (HFO), as well as their applications in various programming softwares - Python, Matlab and Brainstorm.

This means that multiple techniques and subjects will be approached along this dissertation, to represent the full and complete work, and divided into different sections. Although presenting different techniques, all are interrelated by and were developed with one goal in mind: To unravel the possibilities that data analysis and its processing have to offer the modern medical researcher and physician, as well as exploring and developing EEG techniques.

Chapter 2

Background

2.1 Electroencephalography

2.1.1 Concepts and Brief History of EEG

The concepts of electrical potential and electric field had been present since the discovery of current transmission. The idea that this phenomenon could partake not only in so far commonly known charges, solid metal materials, but also in our bodies; did not develop immediately after and demanded further investigation. Created by the different electric potential energy between the body of a neuron and its neuronal branches, the voltage fluctuations of the field reflect the difference in electrical potential during synaptic excitation of the dendrites of pyramidal neurons.

Electrochemical signals, passing from one neuron to the next through synapses, result in electrical fields, that are permanent and ever changing on the brain. Billions of simultaneous signals, in neuronal populations that are aligned geometrically create higher densities in the field, thus becoming powerful enough to reach the surface of the head and can, therefore, be recorded in a non-invasive way by placing multiple electrodes along the scalp.

This procedure is called Electroencephalography, and its recording an Electroencephalogram, or EEG. Its discovery is attributed to Hans Berger, a German psychiatrist who aimed to explore human sensations' mechanisms. In 1929, [10] Berger was able to record electric activity from the scalp of the brain and, more importantly he was able to mathematically prove a connection between the oscillations of the measured electrical field and neurocognitive phenomena.

Naturally, a great breakthrough does not just happen but rather develops from the cumulative sum of previous work done by innumerous others in a cascade of information. Tracing back to the late 18th century, Galvani's, Biologist and Physician, assistant touched a frog's sciatic nerve while performing an static electricity experiment [11]. This accidental movement created a flow of electric current with the leg muscle, that contracted as if living. Current was then able to be detected by a frog galvanoscope, an instrument composed of a skinned frog's leg. That would be used until the end of the 19th century when mechanical instruments were perfected. "Animal Electricity" or Bioelectricity as it would be called later, was one of Volta's inspirations for the studies that led to the discovery of the battery in 1800 [12]. These studies contributed to the understanding of the concepts behind what would one day be the discovery of the EEG.

With the galvanic current, Rolando in 1809, was the first to stimulate cerebral surface and this enabled cerebral localization studies throughout the 19th century (Jackson, Gowers, Gotch and Horsley [13]). The development of the galvanometer and the optimization of the electrometers throughout the 19th

century, mainly by Du Bois-Reymond, Sir William Thompson, L. Hermann and J. Bernstein[14], also led to clearer, more accurate measurements and allowed the conclusion that a "negative potential" was created somewhere on the brain to concede a muscle contraction reaction. This was the first experiment to introduce the concept of action potentials.

By placing unipolar electrodes on either the surface or grey matter of each brain hemisphere, Richard Caton in 1875, was able to identify that the electrical current was definitely originating from the brain; excluding the hypothesis that the brain might only have the capacity to produce motor response to external electric fields. Currents were found to increase with sleep and variations in the baseline unrelated to cardiac or respiratory rhythms were observed. Caton's work was extense and reportedly[13] he was the first Electroencephalographer, performing EEG's on cats, dogs and monkeys.

On the 6th of July 1924, and with all the research previously made, especially the most similar by Caton, Hans Berger, recorded the first human EEG. Through his research Berger also improved EEG analysis, by being able to identify what he called "alpha and beta" brain waves with different frequencies and seemingly related to different neuronal performances.

The concept behind EEG analysis is that, by translating different patterns and intensity of the electrical activity recorded, it is possible to link the recorded EG to recognizable cognitive states. This helps to uncover many practical and academical questions in both patients (such as Alzheimer's disease, epilepsy, Parkinson's disease...) and healthy subjects, as the mapping of the brain or the pathway of a thought.

This was, at the time of the discovery, revolutionary when compared to other methods of neurological diagnosis until the 1970's, when the computerised tomography was able to fill the anatomical spatial hole EEG still left.

The electrophysiological signal can also be seen as a mixture of different frequency signals in distinct wavelengths. The consensual definition of the frequency bands is:

- Alpha - The most common and firstly discovered brainwave, ranging between 8 and 13 Hz frequencies and is found in most subjects in a resting state. This could be while laying with eyes closed or simply resting without a train of thought, for example meditating. Their voltage usually is about 50 and, in its most frequent form, emerges from the from the occipital cortex region.

- Beta - These waves occur at frequencies from 13 to 30 Hz and are recorded mainly from the parietal and frontal regions, while the subject is highly focused on a specific task, like performing a mathematical equation. A beta wave has a lower voltage when compared to an alpha wave.

- Delta - Consists of a larger amplitude wave, with a frequency under 4 Hz. These are very common in infants, where they origin from the posterior region of the brain, but as the subject progresses into adulthood, the waves are only found in deep sleep states, coming from the front region of the brain and in cerebral subcortical lesions.

- Theta - Waves produced with frequencies from 4 to 8 Hz. They normally occur when emotional stress takes over the brain state, in the parietal and temporal regions, in decrease in vigilance and perception or it can also derive from cerebral subcortical lesions.

Other types of waves can be recorded, like μ waves (which technically can be considered an α wave, characteristic of sensorimotor cortices) and γ waves (40 to 60 Hz) but higher frequencies, although existent and studied in the short past, haven't been classified due to equipment signal quality issues. These have all been, however, healthy brain waves opposable to pathologic waves.

The EEG signal is very accurate, as has been mentioned, in a time reference, but since the recordings happen at the scalp, there is a very big noise component associated to the different tissues the signal has to go through and to spatial blurring. The noise, which is in fact an artifact to the cerebral signal, can be from muscle activity, eye blinking or outer body like equipment interference.

Several different methods have been used, in order to help trace back EEG activity to its source. One of the most common, Event Related Potential, manages to lock the EEG recording relative to an event. An event could be refering to an external stimulus or an obvious behavioural reaction. Although widely used, Event Related Potential isn't the sole contender to EEG data analysis.

By knowing the origin and metaphysical relationship to our behaviour, of the EEG's activity produced by an event, we have created a manipulated event, we can use it as prior knowledge data. This can help when overcoming spatial resolution issues with data processing analysis, like spatial filtering algorithms, inverse source modeling analysis or even studying the criticality of brain waves. These techniques will also be further discussed in future sections 2.3.

2.1.2 State of the Art EEG and Miniaturized Electrodes

In an everyday case study or medical use, the routine EEG [15] is performed by placing gel on the head of the subject that reduces impedance thus improving signal quality, directly under the specific positions of the recording electrodes. Up to 264 wet electrodes of silver/silver-chloride (Ag/AgCl) are placed with the help of an EEG cap.

From this information, we should now move on to what actually constitutes a proper EEG measurement: The amplifier, the recording device (usually a computer using a state of the art software), the EEG cap, the abrasive/conductive gel and electrodes.

With improvements over the last few decades [16] including the development of more rigorous high-density recording systems, more sophisticated artifact detection and removal algorithms and improved head models for source estimation - that augment significantly the precision of current estimation - the higher quality of the EEG setup, should naturally be accompanied by its hardware counterpart to allow for a new era of medical acquisition: one that elevates the quality of signal but also does not prevent the patient from a regular day. The miniaturization of the EEG: both in size and weight but also visual perception, seems to be a logical step to elevate the system.

The idea that one could have smaller, miniaturized electrodes, without any sort of cap; came from the team of Dr. Vadim Nikulin et al[1]. EEG is used on an everyday basis at hospitals and in research labs around the world, nonetheless its processing and analysis secrets still linger on.

Spatial resolution is, as was mentioned, still an unsolved problem. On top of this, many neurodegenerative diseases have no predictive factors to their symptoms or can even go by seamlessly to the patient if the seizure or episode isn't perceived. Performing a day-long EEG is the usual practice for some diagnostic cases, such as ascertaining if a seldom or rare occurring seizure corroborates a diagnosis or when investigating how many seizures happen during a day and locate them in space to reach a precise diagnostic plan. This brings about two types of problems with regular electrodes, displayed as was mentioned in the state of the art.

Firstly, using an EEG cap is, without a doubt, not the most convenient nor a seamless way for the patient to proceed with their daily activities. Social appreciation, respect and privacy are considerable parts of our society's way of life.

Secondly, either dry electrodes or wet electrodes may be used. Wet electrodes depend on the gel to decrease the impedance between the electrode and the skin of the scalp[17] [18]. The difference of

impedance between the surfaces tends to rapidly decrease with time of application, but after a period of time it tends to increase. Dry electrodes, on the other hand, when used for more than a couple of hours create bulky creases on the electrode placements, causing head aches and pain.

This leads us to the use of miniature wet electrodes, thus enduring for a longer time without being noticeable on the head of a patient and remaining comfortably longer. The C-electrodes (were C stands for comfort) were developed in an electronics lab, with standard electronics manual tools. With equal quality in terms of frequency range and artifacts to standard Ag/AgCl wet electrodes and proven to maintain mechanical stability up to 9 hours, the electrodes required then development into a commercial stage, to be used firstly by researchers in the fields of neuroscience, rehabilitation and Brain-Computer interface among several other possible fields and even colloquially in the future.

2.2 Epilepsy

The widest definition of epilepsy is for it to be considered a brain disorder characterized by the enduring predisposition to generate recurrent, spontaneous epileptic seizures[19].

Although different types of epilepsy may exist, they share the common feature of reoccurring seizures caused by an abnormally excessive or synchronous uncontrolled electrical discharge from nerve cells in the cerebral cortex. In a very general way, we can divide epilepsy [8] into idiopathic, cryptogenic and symptomatic according to etiology of the epileptic predisposition of the seizure or generalized and partial according to source and diffusion of the electrical discharge. As far as the electrical current discharged is concerned we can classify it in generalized, which implies that the seizures are involving the whole brain at once or partial, also known as focal, since the seizure starts from one confined area of the brain.

If epilepsy is derived from a genetic structure malformation and does not display any abnormalities of the nervous system it can be identified on an EEG is designated as idiopathic, or of no apparent cause. The types of seizures affecting patients with idiopathic generalized epilepsy may include myoclonic seizures (sudden and very short duration jerking of the extremities), absence seizures (often with loss of consciousness) and generalized tonic-clonic seizures (also known as grand mal seizures). However, if the electrical current discharge is focal, seizures tend to be simple partial motor seizures, that may involve the face, or limbs or even multiple unilateral structures; or secondarily generalized (grand mal) seizures.

A symptomatic epilepsy has a specific cause. Injury during birth is one of the most common sources of symptomatic epilepsy. Other than seizures, most of these patients also have neurological issues such as mental retardation or cerebral palsy. Specifically, acquired brain diseases as adrenoleukodystrophy (ADL), brain infections (as meningitis and encephalitis) can also cause symptomatic generalized epilepsy. Symptomatical focal epilepsy is caused by a localized abnormality of the brain, which can result from strokes, tumors, trauma, congenital (present at birth) brain abnormality, scarring or sclerosis of brain tissue, cysts, or infections. This type of epilepsy is often diagnosed based on medical history and MRI scans, albeit sometimes the abnormality is microscopic. It can be successfully treated with surgery on patients who have identifiable lesions. epilepsy without a known source is denoted as cryptogenic.

Although still used by many physicians, due to their use for the past 35 years, the terms of grand-mal seizure and petit-mal seizure have been very recently amended. It is of great importance to keep revising and updating the classification for the detection of epilepsy since it allows physicians to easily distinguish the disorder from others in the utmost rigorous way possible according to newest findings and theories. This essentially helps with establishing the right treatment and prognosis for every specific patient.

The International League Against epilepsy (ILEA)[1] annually revises the terminology and classification associated with the disorder. The following classification is according to their latest review (2017)[20]. The new basic classifications relies on 3 fundamental features:

- Seizure localization - Localizing the separate seizures in matters similar than done by the previous agreement into focal, generalized, unknown and focal to bilateral;
- Level of Awareness - This factor is important for physicians and patients since it helps classify but also determine the level of safety the patient has on a daily basis. It is important to note that awareness is used in place of consciousness due to being easier to classify. A patient can then be focal aware, as in, for example, aware of what is happening although not able to respond; or focal impaired, where the patient has a vague dreamlike idea of the seizure.
- Other features - Other features may be relevant and specific to certain patients, the most common being whether there is movement or not to the seizure.

Figure 2.1: According to the latest International League Against epilepsy's report [8], classifying - which will then help with the correct prognosis - should be done firstly according to the parameter of the onset, then by awareness and lastly whether the seizure is motor.

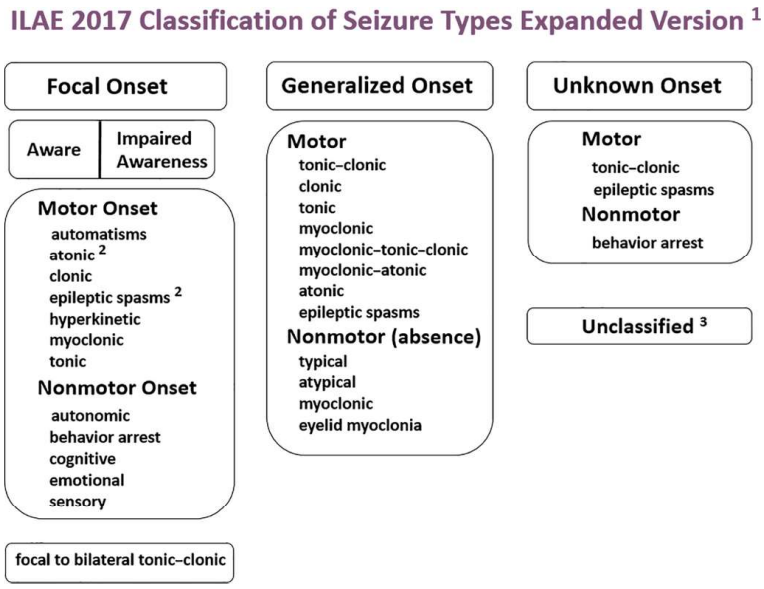

Although the theoretical definition of epilepsy is most widely used, the principle of having two unprovoked seizures more than twenty four hours apart is the most practical and most often used in order to diagnose the disorder. It is also fairly simple to identify typical EEG changes (from a patient's EEG) on an unprovoked patient, which is quite appealing as a first signal towards the epilepsy diagnosis. As can be deducted, epilepsy is not an easy disorder to categorise. Some cases are of unknown source, which most often results in a as probable epilepsy.

As we may have figured out so far, while longstanding efforts in medicine, pharmacology, and psychology brought relief to a number of diseases of mind and brain, there is no permanent cure for epilepsy, yet.. epilepsy can be treated with drugs in order to provide relative stability and some sense of control to its patients. Some are even eligible to undergo surgery, where the area that is causing a seizure is removed, the nerve pathways that the seizure might take are disrupted or even by implanting a controlling device. All of this requires precise knowledge of the source location of the seizure. The common scientific consensus is that augmenting the life quality of patients goes through studying how our brain works and understanding its intrinsical properties, the neuronal dynamics of its being.

Without even mentioning invasive means of brain imaging - which, beyond simply being impractical when conducting an experiment, would also be unethical; there are several non-invasive neuroimaging forms such as is the Magnetic Resonance Imaging (MRI), the functional magnetic resonance (fMRI), the positron emission tomography (PET) or the plain computer tomography (CT). All of these are currently very informative in spatial resolution, however do not allow us to further study the live data, or in other words, temporal resolution, that an EEG can provide.
The combination of both EEG and fMRI - temporal accuracy and functional information respectively - would be a solution to some of these issues [21] [22] [23], allowing for example, a fully non-invasive manner to identify epileptogenic seizure foci [24]. This may be of particular use to identify anatomically complex functional structures while studying their electrical activity in time, such as lobar structures. The mixture of temporal and functional techniques does however introduce some errors that should be taken into account, since the EEG system may provoke an effect on the fMRI signal, and vice versa, when the measurements are taken simultaneously and when the trials are performed separately there can

be no confidence that the integrity of the analysis is maintained [25].

2.3 Data Analysis

Medical diagnostics and medical research in epilepsy have been and will in the near future, benefit from the expansion in methodological capabilities of EEG data analysis and novel methods of artifact removal and detection, thus increasing the precision of source estimation and providing more complete information of both natural neural activity and its perturbations[16]. Several projects of data analysis that are believed to be of relevance for this purpose will now be presented.

2.3.1 Criticality in High Frequency Oscillations

In studies of low range frequencies' oscillations ($<$100 Hz) [26], it has been proven that a higher functioning brain – with an increased dynamic range, information transmission and information capacity – is a brain that works in a critical transitional state between stability and adaptability.

Alike many other subjects, neuroscience's study has been numerous times inspired by other fields. Defining criticality, not in a colloquial sense but rather in its statistical physics meaning – which would be that of a particular type of behaviour subsequent to a system's transition of phase – had its early studies in other fields. Physics, in general, determines the behaviour of a system by separating it into different qualitative phases. In order to distinguish these phases, one may consider order–parameters, quantitative characteristics of the system and study them in relativeness to ambient properties, the control parameters.

This has been done widely in several contexts, for example: in magnets as temperature (order parameter) of iron falls under a critical value, the iron undergoes a change in state, and its behaviour towards other metals changes from paramagnetism to ferromagnetism. When the temperature is precisely at the critical value, in this case the Curie Temperature, the iron and its molecules can be thought of as balanced, maximizing its magnetic stimulus. This balanced condition is something that we can think of when studying brain criticality.

The first studies on a balanced neural network [27] [28] [29] stated that we can establish three phases of function: criticality, subcriticality and supercriticality. Taking a single brain cell as example, balance can be expressed as the capacity the cell has to propagate information onto other brain cells. If the propensity for an action potential to cause another is too high then this process may not be relevant in a sense that it might be subsequent of a specific process, and not entirely due to the cells standard mechanism. If isolated i.e. the propensity for information transmission is too small, a cell would have no relevance at all. These two cases can be classified as supercritical and subcritical. If, however, the propensity for a synapse to occur is exactly 1/N, where N is the number of brain cells, alike the magnet temperature example, a healthy balanced state of criticality is reached between the two states

However, recent views on the subject[30][31][32], have reasons to believe that criticality could, in fact, not be a state that a neuron cell can be in, but a way of work or a behaviour of the cell and it could actually switch from being supercritical to subcritical, being it's transition a way to balance it out. When studying an Encephalogram[33][34], we therefore aim to uncover features that would imply on the functioning of an healthy brain, working on criticality. Doing so through EEG is most often the choice since Electroencephalography is a non-invasive method, therefore free of moral consequences that could come up in an invasive scenario. Working with so brings its own set of specifications[35]: like a poor spatial resolution due to the fact that several artifacts can disturb the signal and lower the signal-to-noise ratio[36]. Such issues can be solved by using higher frequency oscillations, which are spatially more specific. On the downside, this range of frequencies have a lower SNR, thus requiring better quality amplifiers with a lower noise level[26] [30] [31].

Improving the way we look at the mathematical extraction of features, thus interpreting their meaning accurately, is the final challenge. However, describing physiological signals in the most precise manner can be an intricate task since many variables play their part in influencing the signal.

The brain's electrical activity is composed by a complex spectrum, spread over a wide range of frequencies. This means that there is no particular time scale managing the broad distribution of frequencies, no specific upper or lower limit for example. Regular means of description, like studying a mean or standard deviation, do not give a detailed characterization of signals who show no specific associated scale - also known as scale-free. Previous studies [37][38] [39], have shown that power-scale distributions are useful to describe relationships that are not efficiently described by standard distributions. Scale-free signals, like the electrical brain activity acquired by an EEG, can therefore be quantified by their self affinity as a way to measure co-correlation.

That is why the temporal analysis of brain oscillations should go through long-range temporal correlations or other autocorrelation algorithms. Detrended Fluctuation Analysis[40] [**?**] was the first to be described in 1994 by Peng et al.

Undoubtdedly the importance of this and other correlation algorithms has risen in the last decades due to its advantages in categorising methodically complex frequency signals, such as brain EEG signals, in the spatial field. In order to restitute some resolution we can then either construct regression patterns or calculate coherence, a generalization of correlation to the frequency domain[41][42].

2.3.2 Alpha and Theta influence on perception

Before mentioned are the brainwave frequency ranges, commonly divided and agreed upon by the scientific community, of alpha, beta, delta and theta. This section aimed to understand the relationship between human perception and wave activity mainly in alpha and theta ranges of frequency.

It has been shown[43] [44] [45] [46] that alpha and theta oscillations can be linked to human performance when it comes to visual perception. Studies[47] [48] have also established that attention plays a role on brain wave synchrony's functionality and development. Following both those statements, it would be significant to prove the hypothesis that alpha and theta bursts could be directly related not only to our visual awareness but also to self-confidence of the awareness state, that is, to whether one aknowleages and therefore trusts their own awareness.

A study conducted by Iémi et all[6], has shown evidence that alpha power changes detection bias. In a practical way to put it, in trials with low alpha power, subjects tend to see the stimulus more frequently, albeit even in trials without stimulus presentation.

Could it be, and most importantly, could it be proven that the alpha power fluctuates between trials and that it is indeed related to the detection performance? Preliminary analysis suggests that high alpha is related to lower variability of the model itself. What can be said of the theta range of activity during this process? Another question would be if the alpha power is also affecting the sensitivity of the task (i.e., subjects can really differentiate better between the conditions) and even improve their own response with appropriate feedback.

2.3.3 Phase Coupling Algorithm

Modern brain mapping related research and the study of brain functionality goes beyond understanding that multiple zones of the brain can be activated simultaneously, but rather develops from asking the question: how are multiple zones activated simultaneously? What mechanisms lie beneath these connections? What lets our network be correlated and enables this link?

It has been so far established [49] [50] that neuronal communication should rely on the simple anatomical model of proximity when it comes to single cell neurons: an action potential encodes relevant information that is transmitted to the axons of other anatomically near neurons. But, as has been mentioned, not only (not even mainly) anatomical proximity dictates brain activation. A sense of flexibility in the structure of a communications model must be introduced, since a natural cognitive mechanism clearly depends on its function.

Most authors [51] [52] [53] agree that phase-locking patterns of coherence among oscillations are the structural implementation in the basis of neuronal communication mechanisms. This is called the communication-through-coherence (CTC) hypothesis. This hypothesis implies that *"neuronal communication between two neuronal groups mechanistically depends on coherence between them and the absence of neuronal coherence prevents communication"* [49] and is based on the recognition that, while active, neural zones create typical oscillations [54] [55] and that these oscillations modulate a particular rhythm set for that specific oscillation. Rhythmic modulation affects not only the ability for other neurons to spike, but also a neuron's sensitivity to receive synaptic input. This means that communication should lie in the reoccurring rhythm that encodes it and that neuronal groups that oscillate similarly - demonstrating coherent rhythm - are oscillating because they are open for this communication due to their ability to receive input at a particular set of time and related to certain specific activities. Furthermore it has been proven that neural synchronization induces functional activity in several activation patterns, such as the visual, perceptual and somatosensorial areas[51].

Thus, it is determined that the study of phase synchronization, through oscillation coupling is of big importance [56] [57] [58]. Techniques such as Magnetoencephalography (MEG) and EEG, rely on their measurements to deduct the neuronal electrical or magnetic activity produced by the brain, also presented as the inverse problem by several authors [59] [60] [61]. However, and since we rely on discrete sensors to reproduce spatially continuous activity, algorithms developed over the last couple of decades[62] [63] using measures of phase coherence - such as the mean phase value [62], minimum norm, weighted minimum norm, Backus and Gilbert, weighted resolution optimization (WROP), and low resolution brain electromagnetic tomography (LORETA) - do not fully recover the emitted activity as many are not tailored to study phase-locked activities. That is why spatial filters must be further developed in order to identify the less noise inflicted sources and the optimal phase coupling coherences between sensor and source. [7]

PCO, Phase Coupling Optimization includes itself in the spatial filtering type of data driven algorithm once it determines the highest coherence of phase to a desired external variable in order to restore true neuronal electrical activity sources for the discrete sensors available.

Figure 2.2: Phase Coupling Optimization technique as opposed to other sensor space analysis

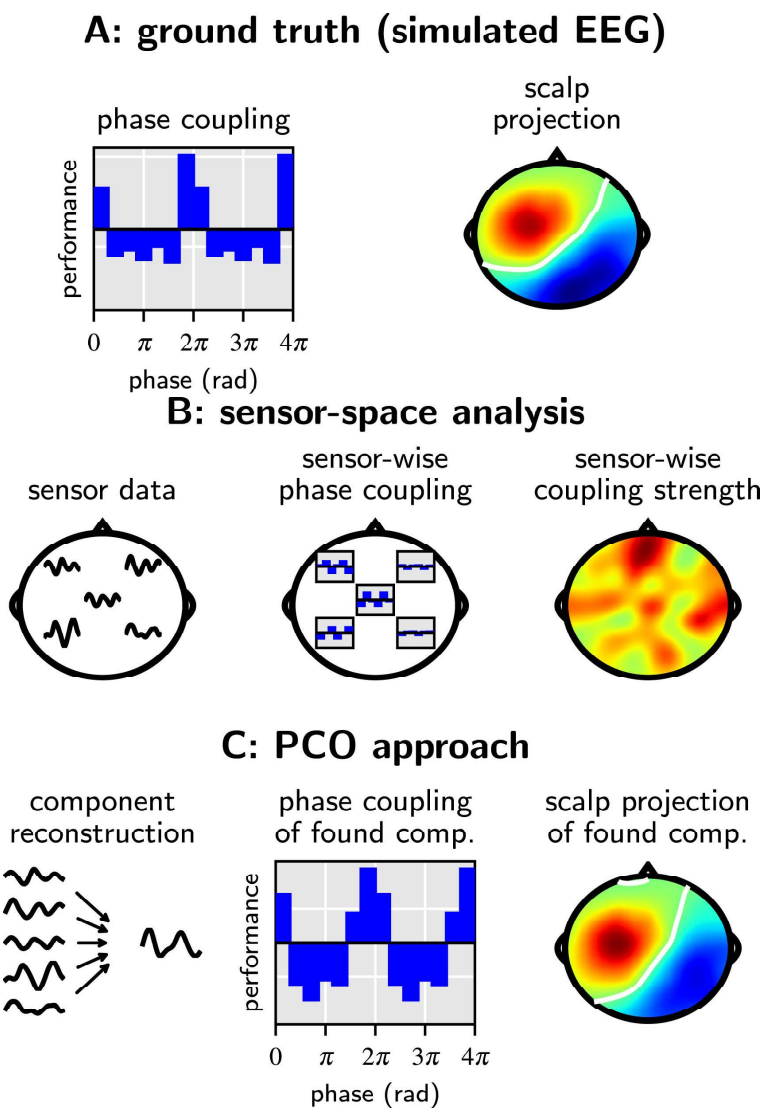

Chapter 3

Electrode Development Stage

Before explaining the methodology, reached by the end of this chapter, we will explore the development process of the physical miniaturized electrodes, in order to provide a complete outlook on the production's procedures and techniques. This will allow a proper understanding of all the choices and arguments that rose regarding each set of the production stage: those would eventually come to be the finalized miniaturized electrodes.

3.1 Production

Initially, and in order to assess the task at hands, approximately 30 miniature electrodes were constructed as described by Vadim Nikulin et al [1]. The procedure consists of:

Preparing the silver ring

- Abrading a piece of silver wire (diameter 0.5 mm, silver content 99.9%) to remove the oxidized layer with a scalpel, perpendicular to the surface;
- From the silver wire form a loop of about 2 mm (using a toothpick to wrap the wire around as a mold;
- Intertwine the two ends of the loop, twisted a couple of times clockwise, until the remaining leg is about 1-2 mm;
- Set aside.

Preparing the copper wire

- Take a copper wire of 0.05 mm width, and with the tip of the scalpel remove the isolation from both end of the wire.
- Attach the copper wire to the silver ring and connector.
- Clamp the electrode ring in a third hand tool, exposing the leg to be ready to solder;
- Using a soldering machine with a fine tip and soldering iron of 0.5-1 mm, solder the tip of the copper wire to the leg of the silver ring;
- Repeat the last step by soldering the other end of the wire to an EEG plug connector.

Electrolysis

- Prepare a beaker with 0.9% NaCL isotonic solution;
- Prepare a 9 volt battery, attached to a coiled piece of silver (such as the one used to make the rings) to the negative terminal, while connecting the positive terminal to the plug;
- Insert the ring into the solution (carefully placing the soldered leg outside) as well as the silver coil for about 60 seconds;
- Let the electrodes set and coat the soldered portions with nail polish as an isolation liquid;

Testing

- Test the electrode on a testing phantom, composed of a textured paper humidified with a NaCl solution of 0.9%;
- Utilise the electrolysing gel to hold the electrode in a random place with a commercial silver reference and ground.

Following this procedure, a couple of problems were identified, related to the manual manufacturing process and surely related to the human nature of mistake. These were small and insignificant troubles when it comes to development of a procedure but that increase their magnitude when we consider commercialization. The issues confine themselves to mechanical instability, whether it is ratio of well produced electrodes - which rose from 1/3 to 1/2 with experience of the producer, but was still far from the ideal result: all electrodes produced being suitable - or the manual handling difficulties created from having millimetric rings with half a millimeter wire to them, these include the breaking of the electrode upon the moment application, from first application to second application.

The main goal was to increase the ratio of working electrodes while ensuring a greater mechanical stability, that would withstand more tension and cable pull - of importance for allowing a longer time frame of usage per session, re-utilization for multiple sessions and an easier application. In order to do this we will take each stage and each step and rethink them according to current literature.

3.1.1 Ring Materials

Although proved that silver/silver chloride rings would be superior when recording bioelectric signals[64] [65] [66] [67], it was decided that for the purpose of a fuller research, one would test Gold electrodes. Besides allowing for a simpler production process, as gold would not need to be electrolysed, gold also has a more stable chemically inert composition to it, and manufacturing miniaturized electrodes with it wouldn't compromise the production costs. Gold electrodes also brought about a different subject: readings of gold manufactured electrodes, compared to the standardly used in a hospital environment (silver/silver chloride electrodes) were completely unreliable once the electronic measurements and comparison of gold and silver aren't compatible. The amplifier used was saturated, making the shown signal irrelevant.

As we can see in the electrode testings section 3.2, unfortunately, the quality between gold electrodes and gold commercially used electrodes did not quite hit the mark set by the earliest comparison's between Silver/ Silver Chloride miniature electrodes and commercial electrodes. The frequency range was not nearly as robust and the noise was much more captured. This led us back to producing Ag/AgCl electrodes, taking now into consideration the next portion of the electrode: the connections to the wire and the wire itself.

3.1.2 Laser Soldering

Initially, the standard procedure was followed to improve the manual technique over time. This, alongside meticulously handling the silver ring - in order to prevent it from oxygenating - was hoped to improve the success ratio. Unfortunately there was no relevant amelioration, many of the connections proved not to be strong enough to endure a good quality between measurements and often became unreliable after testing. An investment from the Charité was granted to promote a partnership with a laboratory at the Virchow Charité Campus, the Charité Centrum Wissenschaftliche Werksttätten (CWW) which would receive the rings and perform the soldering of the miniature ring with the copper thin wire by using a microscopic soldering system. This relationship proved fruitful and assured the desired quality and mechanical stability, in the end, the racio of working successful electrodes increased from 1/3 to 4/5.

3.1.3 Electrolysis

An electrode acts as a conductive point whose surface is the location where oxidation-reduction equilibrium is established. The electrode can either be an anode or a cathode, depending on whether it is receiving electrons (becoming oxidised) or providing them to the other surface. When enough atoms or molecules reach the surface of the electrode, the solution in which the electrode is placed into, donates electrons. This causes the atoms/molecules to become positive ions.

A Silver/Silver Chloride(Ag/AgCl) electrode consists of solid silver that precipitates a salt in the solution which participates in the electrode reaction (AgCl). This enables the above described oxidation-reduction equilibrium that allows the electrons to flow in and out of the electrode system, also known as a "salt bridge".

$$AgCl_{(s)} <=> Ag^{+}_{(aq)} + Cl^{-}_{(aq)} \tag{3.1}$$

The process of electrolysis chosen by the authors of the first electrodes demonstrates a clear preference for a simple methodology since to produce Silver/Silver chloride electrodes by using Sodium Chloride (NaCl) as a solution, is easier to manipulate in regular conditions. By regular conditions it is considered a simple work environment, with no gas isolation for example.

Potassium Chloride (KCl) and (HCl) were considered as opposed to NaCl, since they were highly recommended by many authors, due their Ionic transport number, colloquially mentioned as just transference number, being higher than NaCl. This is relevant since this number represents the percentage, or fraction of total electrical current carried by an ion in an electrolyte mixture. The ionic transport number of the Na+ ion in a solution is about 0.40, while the transport number for K+ and H+ ion is 0.49 and 0.8, respectively. Hence, NaCl takes up a longer time to acquire stability, carrying less current than the K+ and H+ ions, making HCl is the best option for the electrolysis.

Electrolysis times were also rethought. While the initially procedure used a 9V battery for a minute, the sources varied in this type of information and were often inconclusive due to their different statements. Nonetheless, it was clear [optimum electrolytic chloriding of silver electrodes, platinized silver chloride electrode, chlorided silver electrodes]that when aiming for the lowest possible impedance, chloriding should not be carried beyond a certain point.

Adapting the knowledge from previous case studies [17] [18] [15] lead to the conclusion that the chloride deposit should range between 100mA.sec/cm^2 and 500mA.sec/cm^2. With a ring with 1 mm diameter and 0.25mm width, it is expected an area of 0.123 cm^2. With the amount of current density provided by a 4.5V battery, the process should be almost instantaneous and not last longer than 50

seconds. Some sources mentioned that there should be an "electric cleanse" of the electrode, by switching the battery anode and cathode ends before the procedure. This was also implemented onto the final procedure.

3.1.4 Peripherals

In order to make a stronger ring, without compromising its quality, it was early on decided that a plasticized copper wire of about 1mm would be attached to the thin copper wire that is connected to the ring. This would allow some pull on the cable on the EEG plug end, which could be concealed by clothes or even a backpack and still permitting an invisible look as the miniaturized copper wire would still be invisible on the hair.

This comes with its own two disadvantages, more manual soldering to compromise the connection and a harder time preparing the subject since the wire would be longer. Nonetheless, the plasticized wire would have a colour, permitting the specialized technician to better identify which electrode position is which such as in commercial electrodes. Therefore the disadvantages were believed to take less significance than its advantage and hence installed.

Several electrolyte gels and preparation methods were tested. As far as gels go, we were looking for an invisible gel, otherwise it would ruin the purpose of an invisible miniaturized electrode, that would stick hard enough to enable bioelectric signals to be recorded for several hours but also soft enough to allow removing the electrodes without breaking them upon removal – this had happened several times with the initial procedure, the gel would solidify onto the miniaturized electrode and the tension made by the removal from the scalp would set apart the electrode ring from its copper wire.

The preparations encountered went from manual applications, to metal tweezers and finally to plastic tweezers (that wouldn't scratch the ring). Holding the ring in place first and apply the gel after, applying the gel to the scalp and then placing the ring in it, soon became splitting the amount of gel between the desired electrode placement and the actual electrode which would form a glue between them.

Several tools, as were the application rings were actually helpful enough to such a time consuming preparation.

3.2 Testings

In order to compare the several materials and methods, they were methodically combined and tested. Firstly different materials: Ag/AgCl a real EEG test was performed – with this expression it is meant that the data was obtained by placing the electrodes on a subject's head.

The materials used in the test were silver/silver chloride hand-made, gold hand-made and silver/silver chloride commercial. By experience, the gold electrodes' data seem less affected by artifacts after a period of settling of the signal, therefore there are two measurements with gold electrodes 1 and 2, separated by 30 minutes in time.

The electrodes were placed at the positions: Cz, F3, F4, C3, C4; respectively their channel names. All signals were sampled at 2560 Hz sampling rate, in order to meet the recording software, BrainVision's, standard criteria for processing.

Taking a first look at the data, as it would be presented in a clinical environment, with a bandpass filter ranging from 3 Hz to 70 Hz, we can compare the signal of the commercial electrodes with each individual test.

Figure 3.1: In this figure we exemplify a 10 second cut of the signal for a commercial electrode, such as one would use at a regular clinical environment, attenuated for under 3 Hz and over 70 Hz to exclude exterior artifacts.

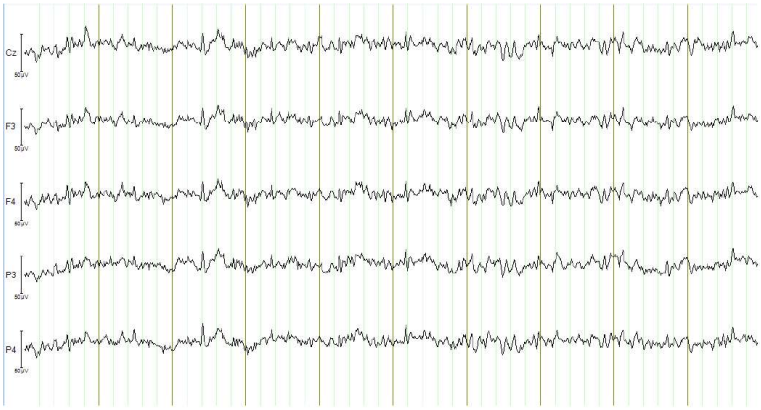

Figure 3.2: In this figure we present a 10 second cut of the signal for the first gold data sampled, right after the placement of the electrodes with the before mentioned filtering

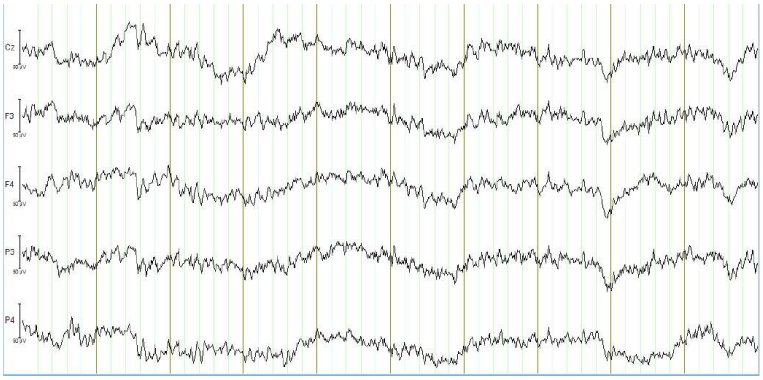

According to most sources [65] [66][67], the gold electrodes' data seem less affected by artifacts after a period of settling of the signal, therefore there are two measurements with gold electrodes 1 and 2, separated by 30 minutes in time.

Actually, it can even be mentioned that in the last graphic, in wich Cz is given as an example, there

Figure 3.3: In this figure we present a 10 second of the signal, this time for the second gold data sampled, which takes place 30 minutes subsequent to data1 of the gold electrodes having had the same filtering

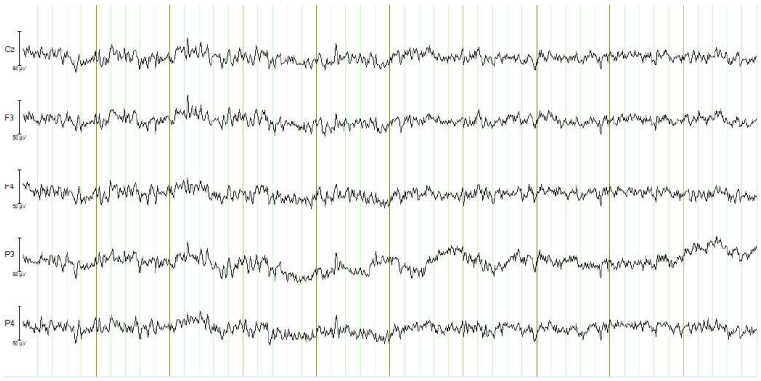

Figure 3.4: Regarding now the silver electrodes, we can see a similar cut of 10 seconds of a signal, filtered in order to caption a realistic clinical environment

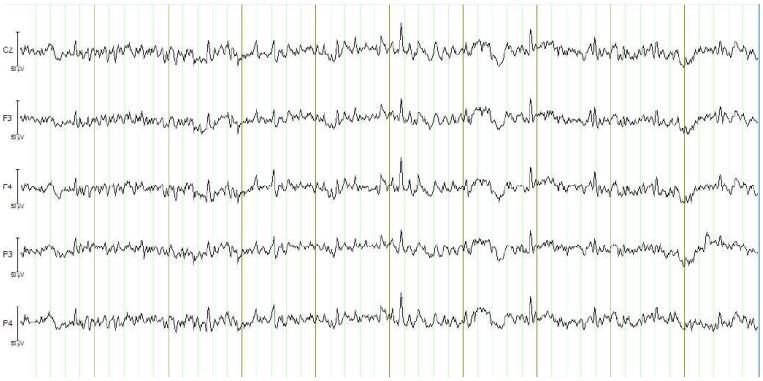

Figure 3.5: Resume and comparison of all the previous graphics only for the Cz electrode (chosen as example)

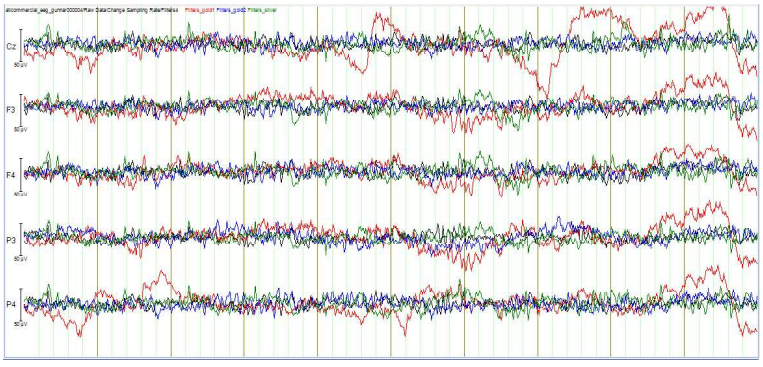

is quite a good level of resemblance between tests. Here we can also see the value of a second sample for the gold setup, appears definitely similar to the commercial and silver samples when comparing with the first data taken (The red line is clearly more unreliable in terms of amplitude and baseline stability).

We aim now to prove that the spectrum of frequencies is truly comparable. A built-in Welch average periodogram, calculated with a Hamming window is applied to all samples, that here are shown on a logarithmic scale for density of amplitude. We can see that the baselines, although not overlaid, are substantially similar and set on 1000 μV/Hz.

Figure 3.6: Spectrum comparison of each channel for every material

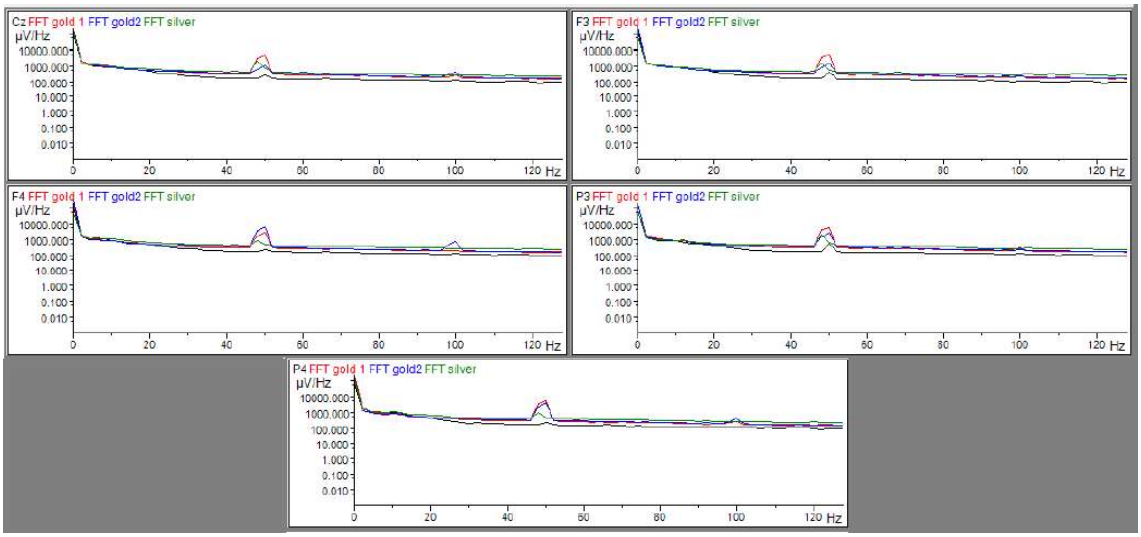

We can also see that the spectrum peaks commonly on the 50 Hz mark, the mains hum [68] noise of the power supply that would easily be filtered out for an actual measurement. Although a common feature, it is also clear, for example in 3.7, that both the standard electrode (represented by the black line) and the silver electrode (represented by the silver line) seem to be less affected by the mains hum interference and therefore provide a better general shielding to exterior noise. This is, of course, a clear advantage of the silver electrodes over the gold electrodes, which contributed if not lead, to their choice as the material of usage in the final method of manufacture of the electrodes.

Figure 3.7: Spectral density for the P4 electrode for 10 seconds of recording for all electrode types.

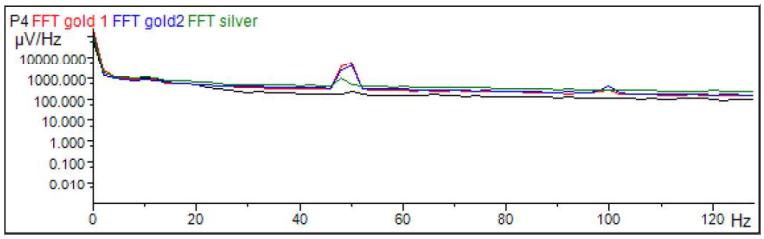

Chapter 4

Methods

4.1 Miniaturized Electrodes

4.1.1 Electrode Production

The production stage of trial and error for electrodes led to the construction of over 100 electrodes with multiple variations in their process. The electrolysis and laser soldering were the areas who underwent biggest modifications in order to improve electrode signal quality and efficiency; but the cable production was also modified to improve practicality. Overall, it is relevant to underline that the partnership with CWW was of vital importance since they enabled the use of more complex techniques, unattainable by simple manual production. As well as research, trial and error were also important to understand and optimize the construction of the electrodes and their procedure. The final miniaturised EEG electrode procedure is as follows:

Preparing the silver ring

- Taking a small piece of silver wire - diameter 0.5 mm and about 4 mm length with a silver content of 99.9%) - the oxidized layer is removed with a scalpel, perpendicular to the surface;
- The wire is bent in a loop form, enabling the two ends to join in a leg of about 1mm length;
- Set aside.

Preparing the cable

- Take a copper wire of 0.05 mm diameter and 30 cm long, and with the tip of the scalpel remove the isolation from both ends of the wire;
- Take a plasticised copper wire, with 2mm of diameter and 30 cm long, and remove the plastic from both ends, exposing the copper wire;
- Using a soldering machine with a fine tip and soldering iron of 0.5-1 mm, solder the tip of the copper wire to the copper tip of the plasticised cable;
- Set aside.

Laser Solder

- By using a soldering micro-laser, solder the already formed ring's leg.

Electrolysis

- In a fume cupboard, prepare a beaker with 0.9% HCL isotonic solution;
- Utilising a specially devised power pack attached to a coiled piece of silver (of the same composition as the ring silver) on its positive terminal, connect the negative terminal to the plug to electrically clean the electrode;
- Insert the ring into the solution (carefully placing the soldered leg outside) as well as the silver coil for 5-10 seconds;
- Remove the ring from the solution;
- Switch the positive and negative sides to perform the electrolytic chloriding;
- Insert the ring into the solution (carefully placing the soldered leg outside) as well as the silver coil for a maximum of 40 seconds;

Final Composing

- Attach the ring and cable to the connector;
- Using a soldering machine with a fine tip and soldering iron of 0.5-1 mm, solder the remaining exposed tip of the plasticised copper wire to an EEG plug connector.

Testing

- Let the electrodes set and coat the soldered portions with nail polish as an isolation liquid;
- Test the electrode on a testing phantom, composed of a textured paper humidified with a NaCl solution of 0.9%;
- Utilise the electrolysing gel to hold the electrode in a random place with a commercial silver reference and ground.

4.1.2 Electrode Trials

Ten miniature electrodes were completed following this procedure and experimented on 3 individuals. One of the subject's recordings was excluded from analysis due to a technical malfunction. To record the physiologic occipital alpha base rhythm, subjects sat in a comfortable chair with arm-rest, their eyes closed and the electrodes were placed using a 64 electrode cap as a referecence for positioning, as shown on 4.1. Along side standard Ag/AgCl EEG electrodes, used for medical purposes at the CharitÃ© Hospital of Berlin.

Both subjects, a male and female, respectively 34 and 24 years old, participated in offline experiments with 15 minutes of rest condition, 10 minutes of self-paced movements and 10 minutes of median nerve stimulation (according to the methodology developed by [4]) with 3.147 Hz as stimulation frequency.

Figure 4.1: The electrodes, both the miniature and standard were set at the blue placements, on positions FC1, C3, P1 and P5; with the objective of recording the occipital alpha rhythm of the subjects and comparing the process for both electrodes. A distance of one to two fingers between the electrodes in each placement was considered, in order to prevent electrode gel bridging. The left mastoid and right mastoid were taken as reference and ground positions, respectively.

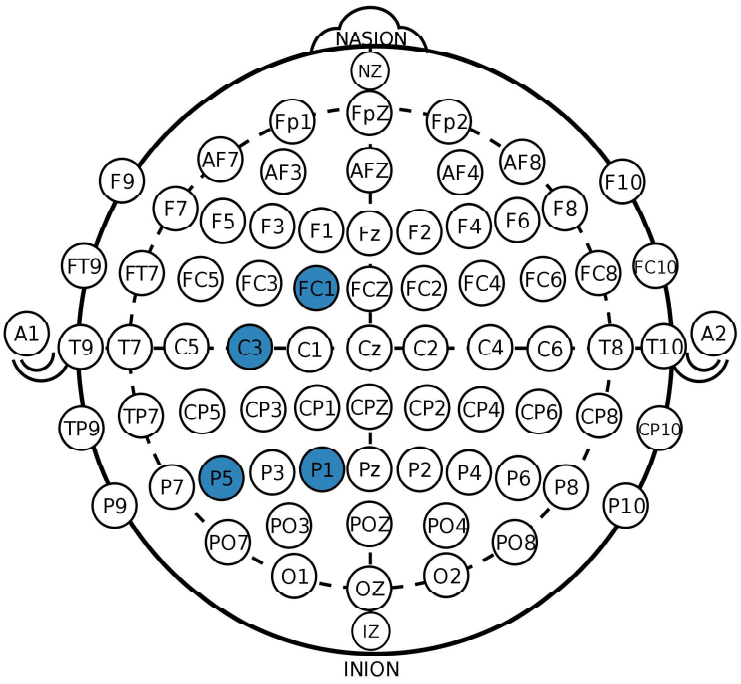

Another subject, subject 6, was considered for this experiment, a male subject with recurring epileptic seizures, interned at the Charité Hospital. This patient's data was unfortunatelly discarded. However some conclusions could be drawn from this trial, that was composed of 15 minutes of a simulated rested condition, where the subject was prepared in the same manner than the above mentioned subjects.

The data was recorded and analysed after the experiment using the open source cross-platform integrated development environment Spyder for Python 2.7 .

4.1.3 Electrode Analysis

Taking into account that the subjects had eyes closed for the duration of the trials or had to stand still - while not minding muscle twitching - the first 10 seconds of every recording were removed in order to allow the subjects to prepare and be comfortable throughout the duration of the experiment.

The signal is addressed by estimating the power spectral density recurring to the Welch Method [69]. This method is preferred to others (i. e. Bartlett Method) since it overlaps the windows used up to 50%, although this slightly lowers the frequency resolution it also reduces noise to the signal.

The Canonical Correlation Average Regression is applied as described by T. Fedele [70], (and whose detailed description is further explored in 4.2 for the *Criticality in High Frequency Oscillations* section of this work) as a measure for cross-correlation between the two populations of standard and miniature electrodes' EEG signals to test the significance of their similarities.

4.2 Criticality in High Frequency Oscillations

The data used for this study was conducted in 2016 [5], having recorded ten healthy subjects' EEG signals, ranging from high to low signal-to-noise ratio (SNR) for the σ-burst, for 5 sessions each. The subjects were instructed to keep their eyes open and to remain still in a comfortable supine position on a bed. The measurements were recorded in a shielded room, with a low-noise amplifier with 10k sampling frequency, built in order to accommodate specifications needed for high frequency oscillations [71] , and 29 Ag/AgCl-plated standard ring electrodes were placed on areas above the pre- and post-central cortices, contralateral to the stimulations, with reference at the nasion. The somatosensory evoked potentials were achieved by stimulating the median nerve at the wrist at a 4.3 Hz frequency, so that a twitch of the thumb was visible for each stimulus.

First of all, it is important to mention that all analysis of EEG, either in Matlab and or Python was supported by the install and use of functions in the toolbox: MEET (`https://github.com/neurophysics/meet`). This toolbox was developed by Gunnar Waterstraat and it encompasses but is not limited to the implementation of canonical Source Power Correlation analysis (cSPoC), EEG interpolation, EEG manipulation and binary reading, IIR Filtering, Spatial Filters, Spherical spline interpolation and CSD, S transform (time-frequency transformation) among others that facilitate EEG reading and its processing analysis.

When working with usual tests, with a well defined scale, it is often standard procedure to apply a mean and standard deviation (or some small specific variant). Supposing that our brain electricity, as previously mentioned in 2.3.1, would better be modeled as a signal system with a Long Range Temporal Correlation (LRTC). As high frequency oscillations are generated by cortical spiking activity and we are probing the excitability of the cortex by applying our stimuli. In theory, the LRTC in high-frequency oscillations can tell whether the excitability of the cortex is in a critical state.

As mentioned before, LRTC can be easily quantified by employing a scale free algorithm as DFA. Hardstone et al[72] summarise perfectly the conductive line of thought of this algorithm:

1. Compute the cumulative sum of the time series to create the signal profile.
2. Define a set of window sizes, T, which are equally spaced on a logarithmic scale between the lower bound off samples and the length of the signal.
    a. For each window length t$\in$T:
        a.i. Split the signal profile into a set(W) of separate time series of length t, which have 50% overlap.
        a.ii. For each window w$\in$W:
            a.ii.1. Remove the linear trend(using a least-squares fit)from the time series to create w detrend.
            a.ii.2. Calculate the standard deviation of the detrended signal, σ(w detrend).
        a.iii. Compute fluctuation function as the mean standard deviation of all identically sized windows with equation 4.1:
3. Plot the fluctuation function for all window sizes, T, on logarithmic axes.
4. The DFA exponent, α, is the slope of the trend line in the range of time-scales of interest and can be estimated using linear regression. The exponent can be interpreted as defining an uncorrelated sequence for α= 0.5, an anti-correlated sequence for 0 $<\alpha<$0.5, or a Long-range temporal correlations for 0.5 $<\alpha<$1.

$$F(t) >= mean(\sigma(W)) \tag{4.1}$$

All of these α estimators of the Hurst exponent, which is the should be modeled as stationary processes. According to the definition seen in the literature [72] [73], a process a process X(t) is stationary if the distribution of X(t) is independent of t, the joint distribution of X($t_1 + \tau$) and X($t_2 + \tau$) is independent of τ and similarly â for all k â for the joint distributions of X($t_1 + \tau$) to X($t_k + \tau$). If, however, the underlying process is non-stationary, it can be modeled as a Brownian fractional motion. In this case, the α estimator of the Hurst exponent should fall under the 1 $<\alpha <$2 range of values.

When α is between 0 and 1, x has been created by a stationary process and can be modeled as a Gaussian process with the Hurst exponent equal to its estimator and H= α. If α is between 1 and 2 then x was produced by a non-stationary process, and H= α-1.

Canonical Correlation Analysis (CCA) is often used to find the most correlated projections between the measurements and the sources. Using the MEET package we apply a form of Canonical Average Regression, developed by Waterstraat et al [4] and previously by Fedele et al [70] by inputting X and Y, two multivariate datasets:

$$X = (X_1 X_2 ... X_N) \tag{4.2}$$

$$Y = (< X >< X > ... < X >) \tag{4.3}$$

Where:

$$< X > = \frac{1}{N} \sum_{i=1}^{N} X_i \tag{4.4}$$

It is crucial to accurately characterise the temporal and spectral content of a signal, therefore it is then defined a time frequency decomposition by applying an S-transform according to the latest literature [9] [74] [75], a variant close to a Discrete Fourier Transform that provides consistent time-frequency portrayal through an entire spectrum, thus obtaining progressive resolution; all the while using a sinusoidal basis function, a shape that encompasses many biological signals.

The S-transform is also custom-sampled in order to adjust the bins to the data, and at least four temporal bins are assigned per cycle. In order to select a subset of series of samples for an FFT calculation, a Hann window function is applied. This particular function is a transformation of the rectangular function window, and specificaly chosen due to its low aliasing effect during the fourier transformation, by widening its main lobe. The Hann window function can be defined by:

$$w(n) = \sin^2 \frac{\pi n}{N-1} \tag{4.5}$$

Where n the number of samples and N the number of bins or subsets.

Figure 4.2: Adapted from [9], this figure depicts a visual approach to the Fourier Transform (FT) and the S-transform. We can see a normalized boxcar function, also named rectangular function in (A), and its FT, a non normalized sinc(x) function(B). Furthermore, the alpha domain of the same function consists of multiple of its shifts (C) multiplied by their FT (D), resulting in (E). When a FT is applied to (E) along the v' axis, the S-domain is produced (F).

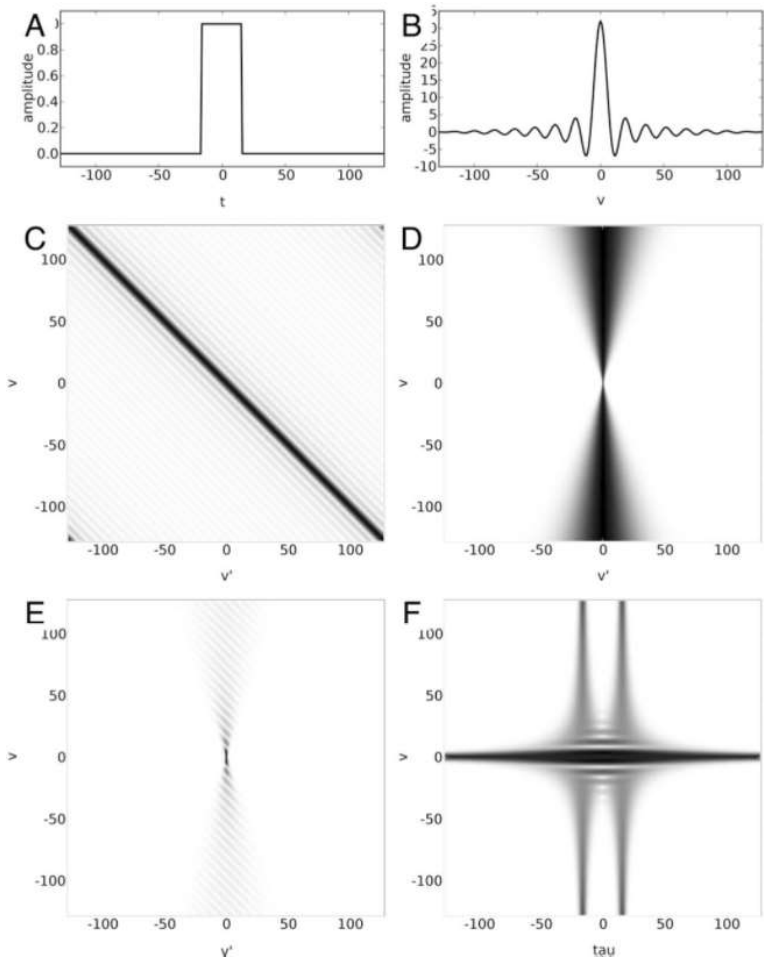

In order to adjust the image's colorimeter's contrast to better reveal the burst, a normalization was calculated by dividing with a pre-stimulus segment of low interest, devoid of evoked activity. This corresponded to the -80 to -20 mili seconds segment.
A Detrended Fluctuation Analysis was then applied in order to determine self affinity of the burst across trials (over time). The mean of exponents was averaged across subjects along each time bin window.

Having the detrended fluctuation analysis and its mean, the noise removal method in this case went through considering a priori knowledge from the dataset. Since it is known that the time window from -80 ms to -20 ms contains no signal (at least no signal of interest), it is therefore assumed to be the baseline of the data. By taking the signal in the before mentioned window and removing it from the whole data, a portion of the noise is removed from the signal+noise, allowing the results to be as trimmed as possible.

4.3 Alpha and Theta influence on perception

As mentioned in section 2.3.2, when presenting the concepts for this project used the data from a previous study performed by Luca Iémi [6] at the Berlin School of Mind and Brain.

This study was conducted for sixty eight patients in total. However the experiment of particular interest to this dissertation was only implemented on thirty three subjects, of which a total of twenty six were pre-processed and analysed.

The participants were placed in a dark room and in 60% of the trials, they were presented a visual stimulus of tilted gabor patches. The remaining 40% trials presented no stimuli. Subsquently they were asked, after each trial, whether they had seen the stimulus: yes or no; but also whether they were sure of their answer. The subjects were given visual feedback on their answers after each trial.

At the Neurophysics group, an analysis was conducted for this experiment by G. Waterstraat. An across-subject Spatial Spectral Decomposition (SSD) is achieved by calculating for each subject the covariance matrices in the 8-12 Hz bandpass and in the 4-8 Hz bandpass. The covariance matrices are normalized by the trace of the 8-12 Hz covariance matrix to have equal weight on the subjects and average the covariance matrices across subjects. The eigenvalue decomposition of the resulting average covariance matrices gives the across-subject SSD. In each subject, using the strongest 10 SSD components, the component power is calculated as root-mean-square (rms) amplitude in the 8-12 Hz window (causal minimum phase filter). The rms-integration is done across a moving 100 ms window (causal, i.e. each amplitude value is determined only by the previous samples). In each sample, component and subject, the rms amplitudes are sorted and binned into 5 bins. For each bin the sensitivity (true positives/(true positives + false negatives)) and the Matthews correlation coefficient was calculated. The Matthews correlation coefficient is a measure qualifies a classification and a value of 0 means random classification, a random of 1 means perfect classification. Note that the Matthews correlation coefficient is not sensitive to class imbalance). In each sample, component, and subject a linear regression of the sensitivity and the Matthews correlation coefficient are calculated. A negative slope signifies that the measure (sensitivity / Matthews correlation coefficient) becomes worse when the alpha-amplitude is increasing and vice versa. In each component individually, a cluster-permutation based p-value is calculated and finally a Bonferroni correction is applied across the 10 strongest SSD components. A very large cluster will decrease sensitivity for smaller clusters. For this specific case, the large post-stimulus significance clusters impeded a sensitive pre-stimulus statistic. Across components, a Bonferroni correction was chosen since distance between the orthogonal spatial patterns is of hard definition.

Similarly to the results presented and described in a next chapter 5.2, a display of the strongest patterns is present here. A threshvalue was set at the absolute value of 0.5 in order to identify automatically relevant patterns for both the alpha wave range and the theta wave range.

In order to better accompany and corroborate this hypothesis, it was then useful to understand more about the probable sources of alpha and theta bursts.

The inverse source modeling was performed using the Brainstorm software to calculate a Minimum Norm Estimation. - Whitened and depth-weighted linear L2-minimum norm estimates algorithm inspired from Matti Hamalainen's MNE software (the full description of the algorithm used can be accessed here [76]).

Figure 4.3: Alpha Wave Spatial Spectral Decomposition

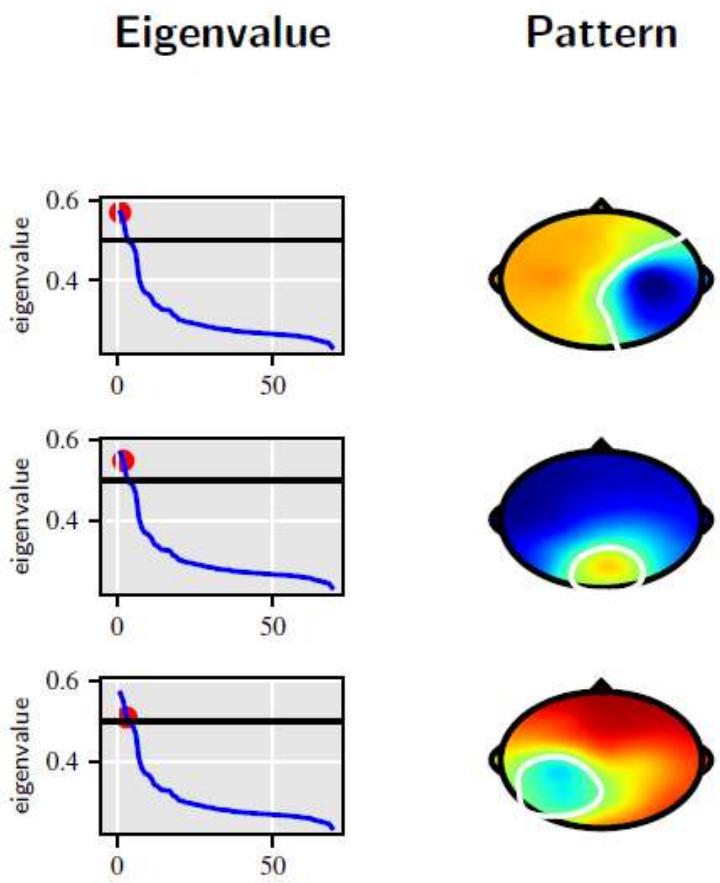

Since there could be several current distributions to explain each electric potential pattern, a possible method to determine them with little to no prior information is the minimum norm estimation. Assuming that the relationship between the source distribution and the electric potential measured on the scalp surface is linear, constituting a lead field matrix, we can estimate it by spatially convoluting the sensor data.

The minimum norm estimation finds a cortical current source density that fits the data by introducing the source covariance as a regularizer, thus solving the illposedness of the situation. Also choosing the L2 norm, the Cartesian distance of the elements of a vector, we constrain our results to the minimum energy norm.

The variant of the algorithm that was used to produce this images was the dSPM, the Noise-normalized estimate [77]. This variant seemed to be of advantage when compared to the simple MNE and to the Loreta noise normalization that Brainstorm also provides by focusing on deeper, more localized sources.

Despite the fact that there are constraints in reality - sources generated in gray matter and pyramidal neurons are oriented perpendicular to the surface, these estimation techniques depend very much on the provided anatomy and other Ã priori characteristics. Here, there is no precise individual electrode locations nor individual anatomical data. The approach chosen was therefore to impose as few priors as possible to the modeling process since the Ã priori knowledge that could be used, would be very

Figure 4.4: Theta Wave Spatial Spectral Decomposition

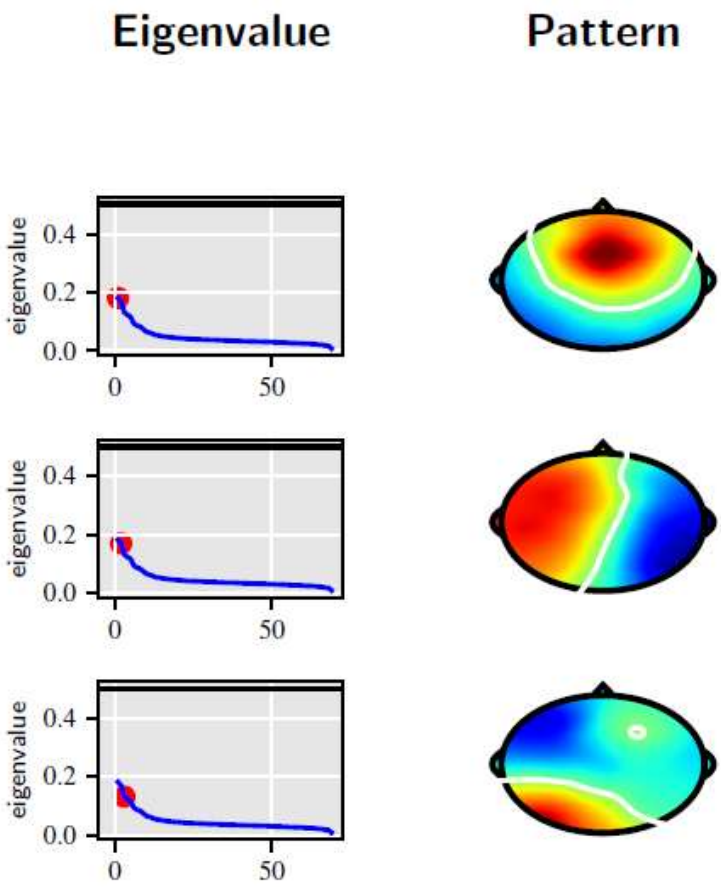

unprecise. This led to the choice of an unconstrained (not constrained to the perpendicular vector to the cortex, otherwise known as normal vector direction) model for all patterns, for both the alpha and theta ranges.

4.4 Phase Coupling Algorithm

Spatial filtering of EEG measurements can be determined by the highest coherence in phase coupling. In this section's background chapter 2.3.3 it was already mentioned that this measure of similarity can be regulated by various algorithms, of which PCO evolved from.

Describing a simple forward model as a linear equation, if N is taken as each neural activity source at a t discrete time, the superimposition of N to each scalp electrode C denotes the sensor-space activity x(t) as:

$$x_{C\times 1}(t) = A_{C\times N} \times s_{1\times N}(t) \tag{4.6}$$

Figure 4.5: Representation of a simple linear forward model with EEG electrode activity as the model's response

where A is a mixing matrix, the effect an electric signal suffers from since it is produced to its measurement on the scalp. It contains the information of the anatomy to which the signal is subjected and external noise absorption. To each column of A: $a_{i\times j}$ should correspond each projection of the source to the scalp, also known as its spatial projection.

A spatial pattern technique is therefore a way to model a filter which would replicate the true mixing matrix's effect to the source-space.

$$s_j(t) = w^T_{C\times 1} \times x_{C\times 1}(t) \tag{4.7}$$

Where s_j is denoted as each t discrete times' individual source activity and w represents its individual spatial filter. The complete matrix of spatial filters, $W_(C \times C)$ is, ideally, $W = A^T$.

At this time, it is relevant to define an well-posed and ill-posed problem. In mathematics, well-posedness is defined as a term to describe a problem whose solution exists and is unique, changing continuously along with its initial conditions [78] [79]. An ill-posed model is one which does not follow these properties.

Since the number of EEG electrodes, the sensors C, will always be severely inferior to the number of electrical brain activity sources N, a considerable number of sources will have their neural activity reach each scalp sensor. This phenomenon is responsible for augmenting the complexity of the received signal and increasing the number of possible pathways, therefore making the problem ill-posed.

Retrieving the most relevant sources to a desired activity is the goal of the PCO algorithm. The property used to quantify this relevance is phase-coupling of the neuronal sources to a specific target activity variable and this is maximized to find the most relevant spatial filters.

The Modulation Index (MI) is one of the ways one can quantify the interaction of rhythms in different frequency bands [80] by computing the difference between an experimental histogram of oscillatory phase vs. target variable deviates from a uniform distribution by calculating the KullbackâLeibler distance, widely used in statistics to quantify the difference between two distributions [81] [82]. Although convenient and broadly used for measuring phase-coupling relationships, this method does not resort to the MI since it doesn't allow for a fast optimization algorithm - due to its non-differentiable nature - and was thus discarded.

Instead the Mean Vector Length (MVL) is used. In the MLV method [83], the phases of an oscillation are combined with the observational target variable. The length of the mean vector of these combination of values will differ from 0 if there is a phase-coupling relationship. This method does allow differentiation of its gradients and therefore a faster optimized algorithm.

Following the PCO method described in [7], the neuronal sensor space $x_c \times 1(t)$ is taken as an imaginary: $x(t) = y(t) + z(t)I$, with $i^2 = -1$ and j as each EEG electrode. The Hilbert transform is applied in order to obtain the analytic signalâs amplitude. Being t_k the time point of each k trial, $\alpha(k)$ is defined as the possible phase dependent univariate target variable for that k trial. A zero mean and unit variance across trials is set for $\alpha(k)$, for normalization purposes. The PCO method maximizes the length of the mean vector of the phases of $x(t_k)$ and $\alpha(k)$ by optimizing a linear filter $w = [w_1, w_2, \hat{a}, w_c]^T$. W is defined by:

$$w = argmax(l(w)) \tag{4.8}$$

$$l(w) = |\frac{1}{K}\sum_{k=1}^{K}\frac{\alpha(k)w^T x(t_k)}{|w^T x(t_k)|}| \tag{4.9}$$

Where $l(w)$ is the de facto mean vector length. The algorithm is trained by running it 15 times with random seeds of w which are verified by temporal permutation tests of $a(k)$. This ensures that connections between the phase of the target variable and the oscillation are not pure coincidence. When the mvl obtained exceeds the mvl of the training algorithm, the source activity is as close as it can be to reality.

Figure 4.6: Visual Steps to PCO [7]

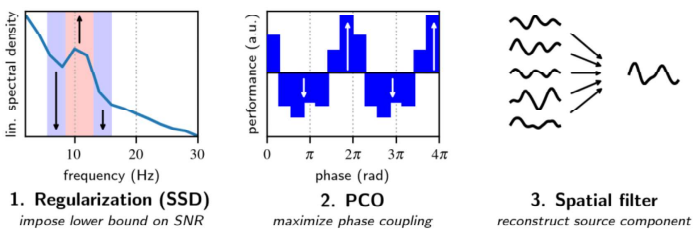

Figure 4.6 represents the algorithm implemented. Firstly, in 1), the SSD regularises the signal by augmenting frequency peaks of interest and lowering the activity in its flanks from the baseline, thus

isolating the peak. 2) PCO finds the maximum dependence of the target variable to the new SSD pre-processed signal phase. 3)The PCO algorithm applies a spatial filter to the data, reshaping the source activity.

This new technique was implemented in matlab and made available at `https://github.com/neurophysics/PCO_matlab`.

Chapter 5

Results and Discussion

5.1 Miniaturized Electrodes

The final electrodes produced resulted in the following prototype.

The electrodes are still invisible to the human eye when placed upon the scalp. The placement of such petite devices is eased by locating them in between hair follicles. This method also reduces resistance between the skin and the metal itself. It was also noted that the appropriate gel, application and removal methods as well as the experience of the technician played an important role in the successful duration of the miniature electrodes throughout trials.

The tougher plastic wire (which can easily be tucked under a shirt or even backpack) allowed a stronger physical stability for the device for the duration of the interval between stimulation sections (about 5 hours) and also endure being removed without breaking

The laser connection of the ring onto itself also stood throughout the testing stage. All of the strengthening methods led to an all around success of the miniature electrodes and their overall mechanical toughness therefore improving their status from discartable electrodes to reusable electrodes.

Figures 5.3, 5.4, 5.5 and 5.6 are periodograms representing the spectral density as calculated with the Welch Method for a random subject for each electrode position, comparing the amplitude of the signal as nano volt per squared Hertz for each frequency in Hertz for the resting state trial.

These figures do not represent the full frequency spectrum but instead a relevant frequency range from 10 to 100 Hz in order to better expose and identify the 50 Hz amplitude spike, which corresponds to noise from the AC supply.

Across every periodogram we can see that the amplitude coincides for both electrode types: standard and miniature. In fact, the miniature electrodes only show less amplitude for the AC artifact spike at the 50Hz, which could possibly mean that they actually are less prone to technical artififact noise as proposed by Vadim Nikulin et al [1].

This section was also useful in order to later interpolate and remove the 50 Hz artifact from further analysis.

Amplitude values for every resting state trial remained between the expected [31] range of 10^2 to $10^4 nV/\sqrt{Hz}$ which vouches for the miniature electrodes' ability to capture the same signal amplitude

Figure 5.1: Electrode Ring Zoom

Figure 5.2: Image depicting the final prototype under the testing phase

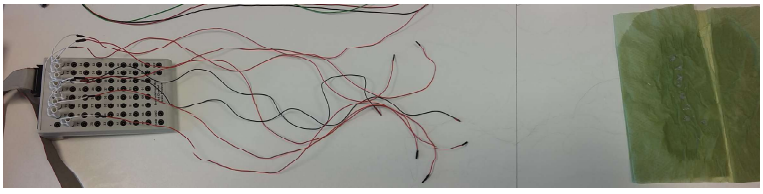

Figure 5.3: Spectral Density Periodogram comparison between the miniature electrode and the standardly used at position Fc1

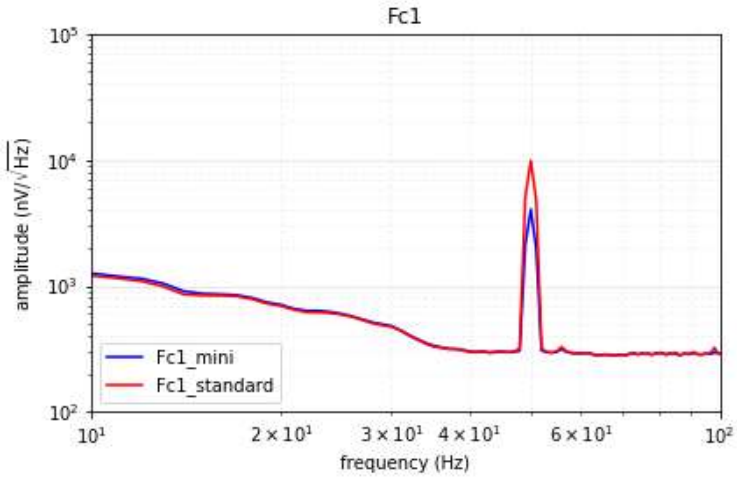

Figure 5.4: Spectral Density Periodogram comparison between the miniature electrode and the standardly used at position C3

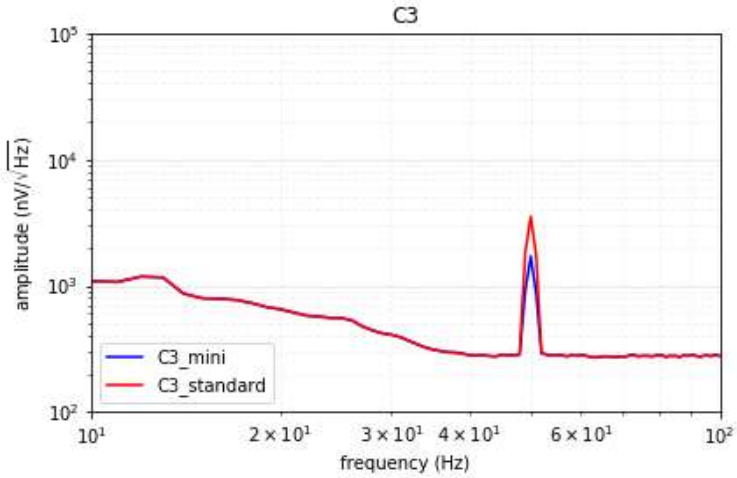

Figure 5.5: Spectral Density Periodogram comparison between the miniature electrode and the standardly used at position P1

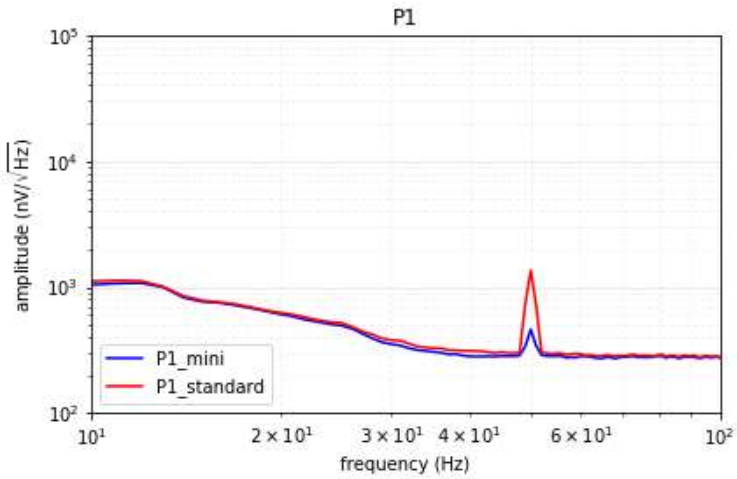

as standard electrodes.

As for resolution of the frequency captured in the miniature electrodes' signal, the stimulation trials were analysed, as previously mentioned in this work, with a view to detect the alpha rhythm burst in the occipital cortex.

It is relevant to also mention that a alpha burst was not found in either electrode type for one of the subjects. This is quite a usual finding since not all subjects experience the same change in alpha waves in the same manner. For the subject where we can single out the change we see that not only the presented burst is similar in amplitude range but also that the filtering technique deployed automatically by the amplifier presents a cleaner result for the electrodes.

The main goal would be to prove that the miniature electrodes are able to be treated and presented as already in use in every hospital.The previously demonstrated results ultimately lead to the optimal conclusion that the produced electrodes perform according to the preproposed standards: in the same range as standard electrodes, maintaining (and arguably improving) the signal quality. The signal processing techniques could be done online or offline depending on the specific demands the trial or experience and other bursts.

Regarding the external subject, already mentioned in 4.1.2, 6, described as a subject with recurring Epileptic seizures. Even though a proper experiment wasn't conducted, it was easily seen by the medical staff that the epileptic seizure's specific signal can also, as the alpha burst, be identified on the output signal from the miniature electrodes, which also can also be taken as future evidence for this device's system as a means of portable, reliable, reusable, invisible, medical diagnosis.

Figure 5.6: Spectral Density Periodogram comparison between the miniature electrode and the standardly used at position P5

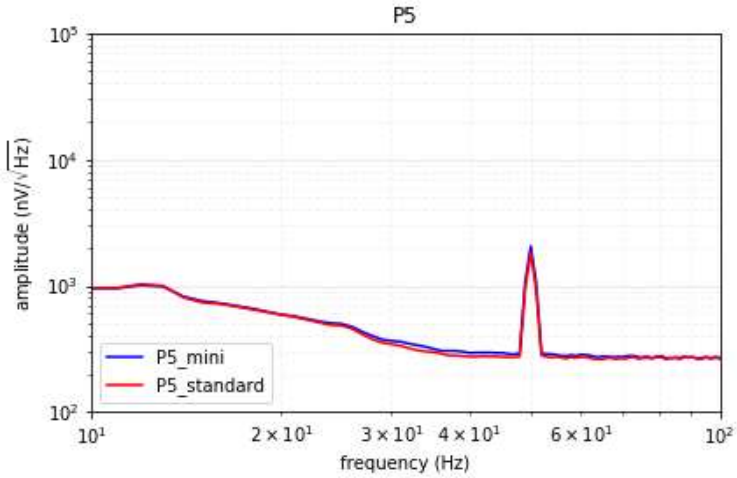

5.2 Criticality in High Frequency Oscillations

With a concise presentation in mind, only results for one of the ten subjects will be included in this section - note that all results are presented in the appendix 6 - as a showcase of the analysis performed for all high frequency oscillations' recordings.

The first image we obtain for the DFA result is figure 5.7,

Figure 5.7: Detrended Fluctuation Analysis

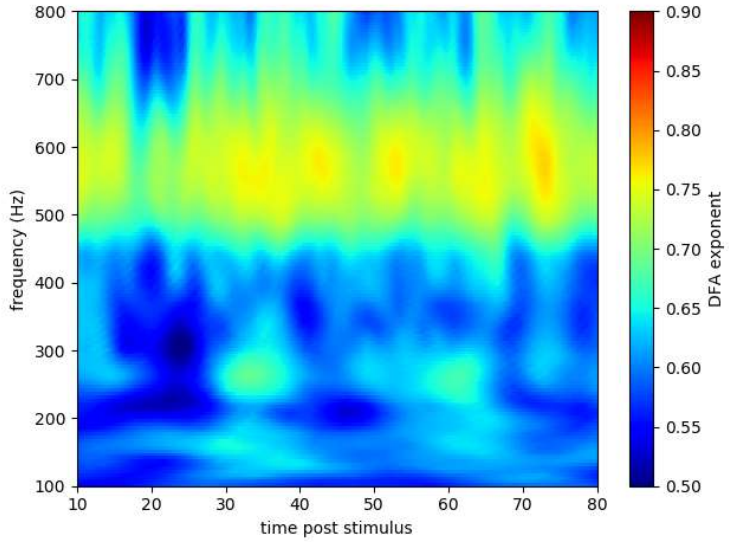

A very high DFA exponent is presented, a burst on the 600Hz band, all through the dataset. This is accompanied with a wavelike fluctuation of values, similar to a sinusoidal wave. At this stage the noise hasn't been removed from the signal, and the method described in 28 is applied.

Figure 5.8: Optimal fit for the LSD

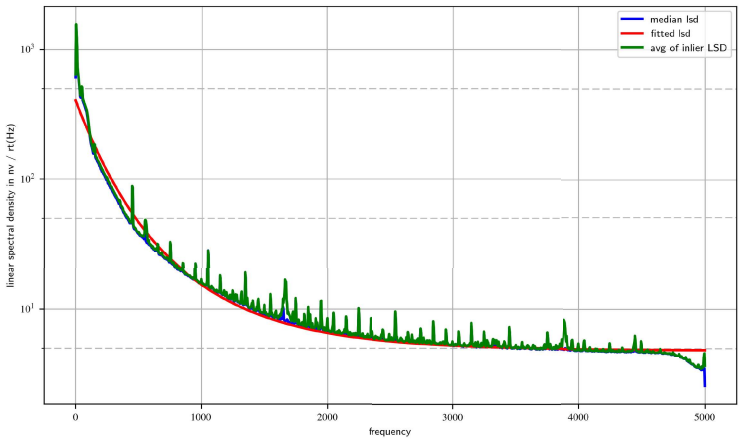

Taking a look at figure 5.8, that represents the median of the Linear Spectral Density (LSD) of non-overlapping 1 second blocks. The stimulation wavelets also need to be removed and the signal interpolated. Comb-shaped artifacts in the bipolar montage were caused by a close-by 3T-MRI device. Remarkably, the proposed analysis proved robust against these interferences. This was performed with a

median fit signal interpolation.

Figure 5.9: Time Frequency Analysis without noise

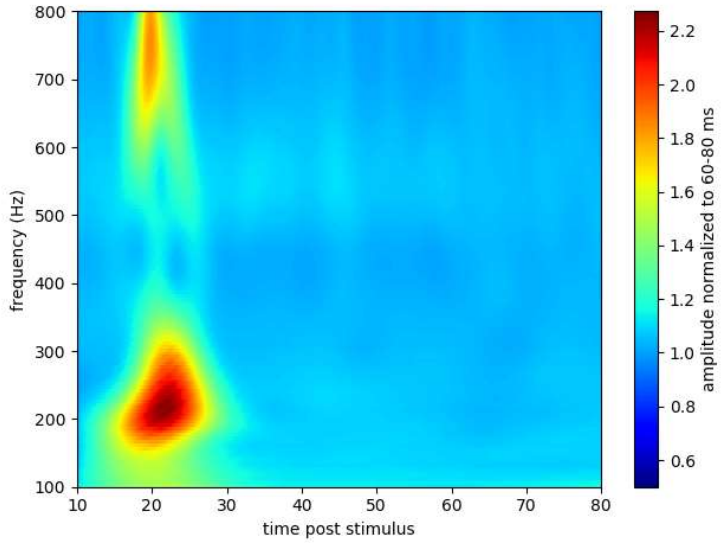

With all the processing applied to the data, the final result is shown in 5.9, where it is now clear that not one, but two points of LRTC can be extracted, both in the higher frequency we had seen in the first view, but also in a lower frequency band. This is, undoubtedly, not relevant unless the exponent is consistent across subjects and calculate its significance.

Figure 5.10: Detrended Fluctuation Analysis Across Subjects

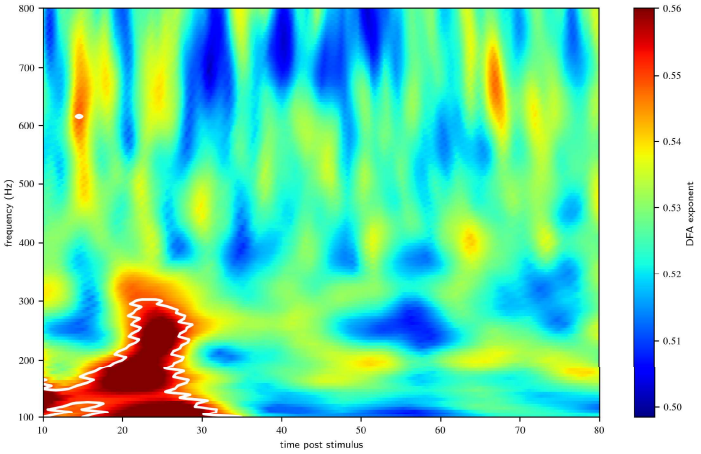

A standard bootstrap significance was applied to all subjects's data (shown in 6) in order to show the statistical importance of the results. This is presented in 5.10 as a white line, revealing that the lower frequency burst is of statistical interest.

A DFA analysis is still, yet not only relevant to identify common bursts across subjects but ultimately to retrieve information regarding the criticality of the brain at the same frequency spectrum. More can be concluded when using this information so that one may feed a CCAvR algorithm and gather valuable information regarding the spatial patterns of the relevant found burst.

Figure 5.11: Patterns of the significant burst

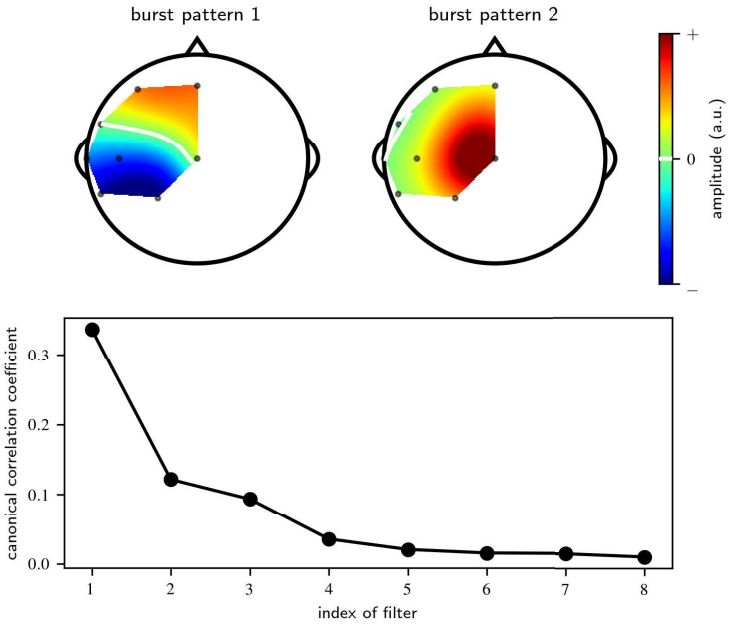

In 5.11 we have two of the patterns resultant from the spatial filter optimization, in which the correlation of single-trials was increased, allowing a focus on stimulus-locked EEG.

The index of the filters in the CCAvR implies that only the two strongest filters are of interest, since they are represented with a higher amplitude relative to the baseline created by the following filters. These were therefore chosen as the most probable pathways.

The strongest filters are independent from one another and, as two independent frequencies constitute a complex signal, these patterns represent the most probable sources of what could in fact be two different, distinct brain cognition criticality processes. It can be seen in the patterns that different polarities are assumed from the first to the second most probable pattern (however these cannot be determined unambiguously); but also that they display rotated bipolar or unipolar patterns.

The most significant filter however, (i.e. the filter ”burst pattern 1”, that corresponded to the highest canonical correlation coefficient) evidences a bipolar configuration above the parietal cortex contralateral to the stimulation site.

5.3 Alpha and Theta Influence on Perception

The calculations from a previous study - SSD results - were fed to Brainstorm.

A conclusion previously reached by the team was that the second pattern, although not mathematically stronger than the first, seemed to accurately describe a visual cortex activation pattern.

Figure 5.12: Patterns of the significant burst

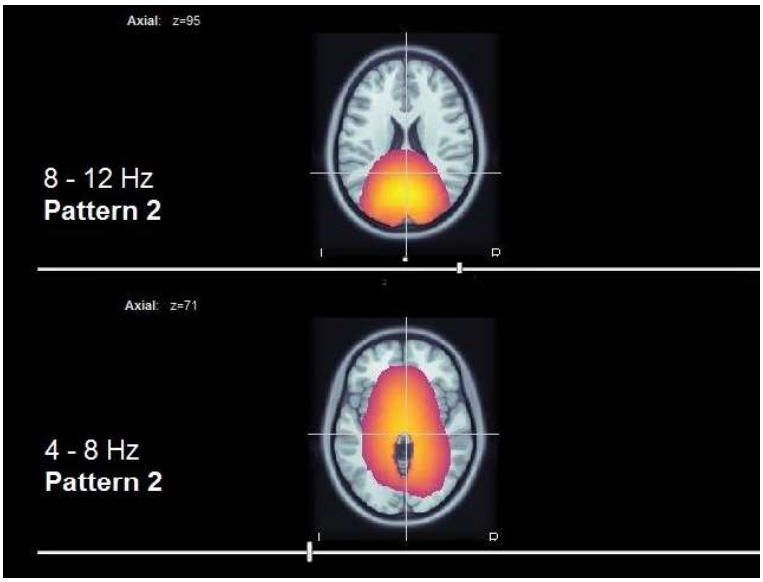

Figure 5.13: Patterns of the significant burst

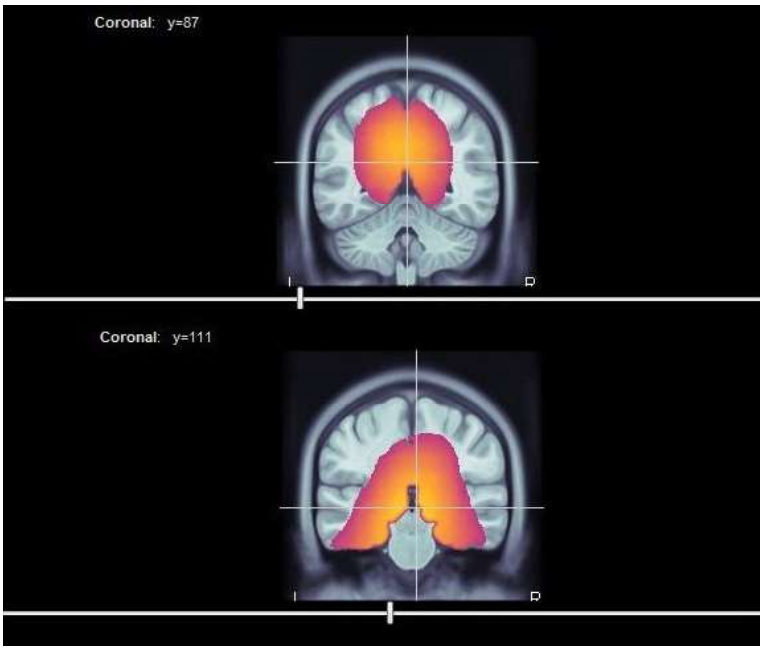

The last 3 figures 5.12, 5.13, 5.14 evidence 3 different image cuts: axial, coronal and sagital views respectively, of the calculated inverse source modeling activation for the second strongest pattern. The top image corresponds to the 8 to 12 Hz frequency range of the data, the alpha range; while the second image corresponds to the 4-8 Hz frequency range of the data, the theta range; for all figures.

Figure 5.14: Patterns of the significant burst

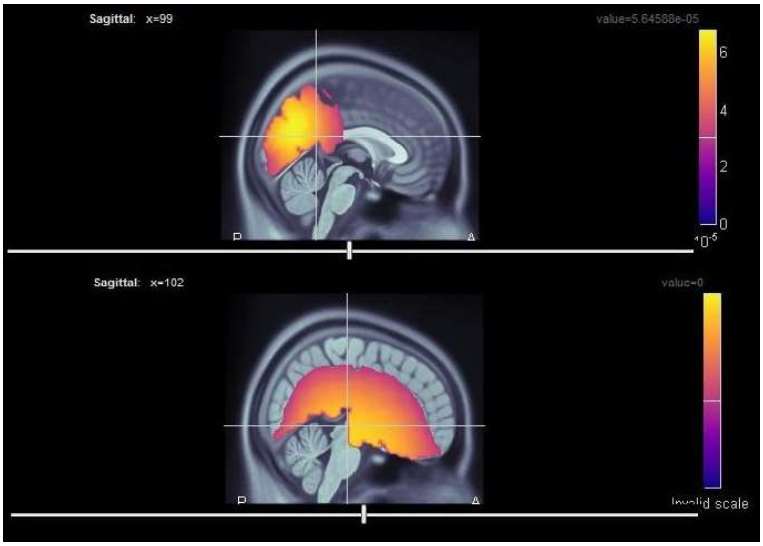

For the alpha wave range, we can see that the occipital cortex is ultimately its provenience local. However, even with the sLORETA approach, which introduced a sharper definition to these results, one cannot contain the inverse source modeling resulting pattern to the occipital cortex.

In the theta range, we can see that the posterior cingulate cortex seems to be a source of activity, which could in fact be accurate and related to the area's visual perception [2] [3].

Another hypothesis may be that this type of analysis over propagates to more internal cerebral locations due to mathematical error: it might be that since the SSD is ran across subjects, the algorithm is coerced to find a compromise between different individual patterns. For instance left and right radial sources might be merged into one showing rather deep dipole. In order to refine this result and prove this hypothesis, the strength of the regularization parameter for the sLORETA algorithm was changed in 5.3.

Figure 5.15: Alpha wave range strength regularization parameter changes for the second strongest pattern

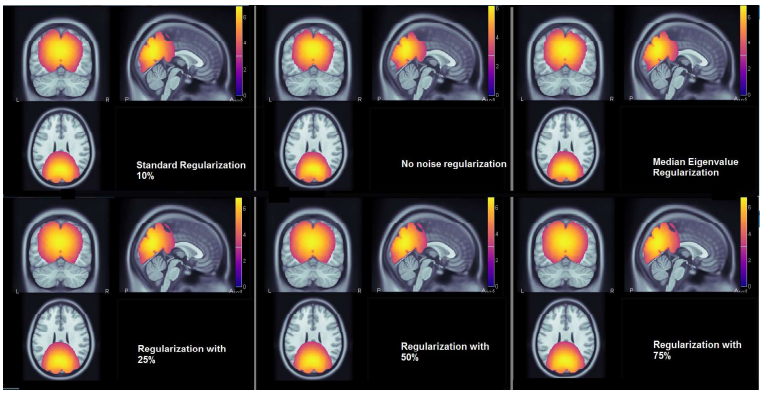

Unfortunately, as can be seen in no visual substantial difference can be achieved be changing this parameter. Future work may come from further analysis towards reducing the diffuse results.

Another approach might be to, taking into consideration what sort of activation pattern one might

find from a visual related task, find the best window towards that goal for the alpha range and inspect what changes for the theta frequency range and vice versa.

Figure 5.16: Best window cut for the alpha wave range

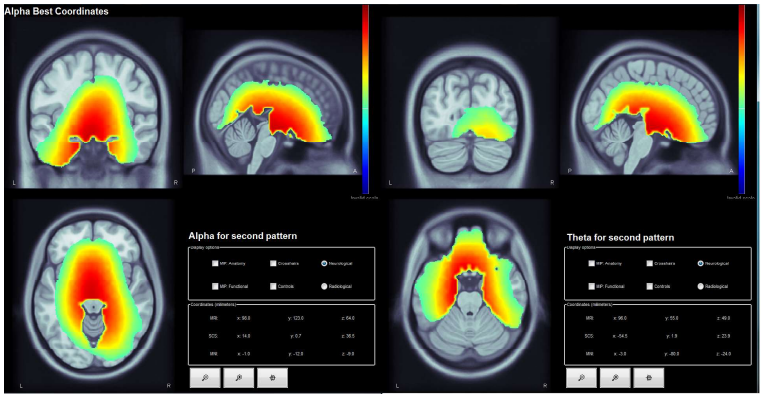

Figure 5.17: Best window cut for the theta wave range

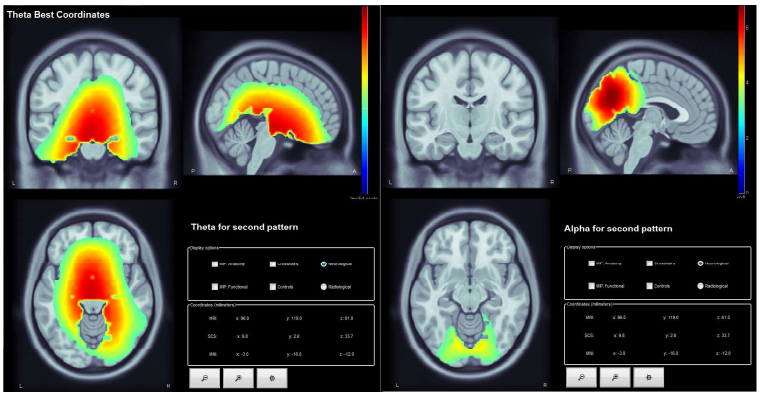

This figure evidences an occipital activation for this specific time window for the alpha range, where we can see that the theta range focuses mostly on diffuse uncorrelated areas while for the best theta activation window 5.17 evidently still shows alpha range activation.

Together with further statistical analysis, it could be concluded, as seen in [84], that the heterogeneous choice model replicated the finding that oscillatory alpha power influences the perceptual bias. Additionally, strong occipital alpha power was found to increase the variability in the detection model. Furthermore, the power of a bipolar theta source, tentatively attributable to a deeper origin, was found to be negatively correlated to the overall sensitivity of the visual detection task.

The SSD effectively extracted collectively strongest sources of alpha and theta activity across subjects, hereby increasing the spatial specificity of the data and the signal-to-noise ratio. The heterogeneous choice model revealed that alpha oscillations not only influence perceptual bias but also the variability in the model and that strong regional theta oscillations are correlated with less effective visual detection, potentially due to drowsiness. However, further studies are needed to characterise the neurophysiological underpinnings of these observations.

5.4 Phase Coupling Algorithm

Sample realistic forward head model simulations, created by [7], were used in order to recover scalp patterns. As described in [7], "randomly placed alpha source exhibiting phase coupling to a synthesized target variable, mixed with 4 randomly placed uncoupled alpha sources and 500 sources producing 1/f noise. The SNR was varied between 0.01 and 2 in 41 logarithmically spaced steps, and for each SNR results were averaged across 10 independent runs of the simulation. All sources were randomly re-positioned and all signals were re-created in every run of the simulation to eliminate a potential bias of incidentally favorable or unfavorable configurations." Examples of a generated source pattern and phase-to-target-variable histogram are depicted in 2.2.

The results found corroborated the values at [7] . For SNRs > 0.5, using SSD as pre-preprocessing, PCO could reliably recover the source patterns with an absolute cosine similarity between the original and recovered patterns > 0.85 for SNRs as low as 0.1 (-10 dB).

Without the SSD preprocessing algorithm however, PCO demonstrated a considerable decay of effectivity for SNRs < 0.5. Additional analyses showed that this was a result of overfitting: PCO maximized the mean vector length even between the phases of band-pass filtered multivariate white noise and an unrelated random variable. SSD reduces the amount of overfitting by imposing a lower bound on the SNR of the examined neuronal oscillations. This effectively prevents PCO from maximizing spurious couplings between noise and the target signal. For very low SNRs, approaching 0.01, this additional constraint on the SNR did not anymore improve the results significantly.

This algorithm could recover both the source pattern of the coupled alpha source as well as the original relation between the phase of the source signal and the target variable with low variability between independent runs (indicated by small SEMs). However, it must be noted, that without antecedent dimensionality reduction, PCO is prone to overfitting. PCO will be a valuable tool to increase the sensitivity of phase coupling analyses and to localize the sources of phase coupling.

Chapter 6

Conclusion

Although not recent, Electroencephalography is still one of the most relevant diagnosis tools for neurological diseases and disorders in medical centers, as well as a research tool in investigation centers around the world. Its accompanied continuous hardware and software updates, regarding not only novel manufacture but also preprocessing and analysis techniques is still pertinent today.

The first aim of this dissertation was to research, develop and implement a miniature electrode that would provide medical centers an invisible EEG system for portable wear of patients, such as epilepsy patients. The goals of the device were for it to require no visible tools, be comfortable for long wear, provide stable signal measurements and impedance without supervision for long wear, be reusable and most importantly, not compromising the signal quality.

The electrodes produced consisted of an Ag/AgCl $\approx$ 2mm ring, lasered to a 0.05 mm diameter copper wire with $\approx$ 30 cm length, secured to the connector by a plasticised 2mm diameter wire of $\approx$ 30 cm length. Ten miniature electrodes were completed following this procedure and experimented on 3 individuals.

These were tested against standardly used Ag/AgCl electrodes, by inducing a finger twitch in subjects therefore inducing an alpha burst in the motor cortex. This effect, as well as the spectrum analysis, produced similar results for both electrode types. The electrodes meet all the criteria imposed as initial goals but nevertheless were tested on healthy subjects. For further studies, an epilepsy patient group of subjects should be analysed with the comfort electrodes in order to establish true medical feasibility when it comes to monitor the condition and even diagnose it.

The second aim of this dissertation was to cover and develop relevant analysis regarding EEG algorithms. Namely, *Criticality in High Frequency Oscillations*, *Alpha and Theta Influence on Perception* and *Phase Coupling Algorithms* were implemented on different study groups.

In *Criticality in High Frequency Oscillations*, a DFA analysis is still, yet not only relevant to identify common bursts across subjects but ultimately to retrieve information regarding the criticality of the brain at the same frequency spectrum.

For the *Alpha and Theta Influence on Perception*, it was noted that, for the alpha wave range, we can see that the occipital cortex is ultimately its provenience local. However, even with the sLORETA approach, which introduced a sharper definition to these results, one cannot contain the inverse source modeling resulting pattern to the occipital cortex.

In the theta range, we can see that the posterior cingulate cortex seems to be a source of activity, which could in fact be accurate and related to the area's visual perception [2] [3].

The SSD effectively extracted collectively strongest sources of alpha and theta activity across sub-

jects, hereby increasing the spatial specificity of the data and the signal-to-noise ratio. The heterogeneous choice model revealed that alpha oscillations not only influence perceptual bias but also the variability in the model and that strong regional theta oscillations are correlated with less effective visual detection, potentially due to drowsiness.

The *Phase Coupling Algorithms* implemented on Matlab could recover both the source pattern of the coupled alpha source as well as the original relation between the phase of the source signal and the target variable with low variability between independent runs.

All these analysis' contribute to a ground knowledge of the EEG signal and its interpretation shows valuable insight to future neurocognitive and neurodynamics paradigms.

Bibliography

[1] V. V. Nikulin, J. Kegeles, and G. Curio, "Miniaturized electroencephalographic scalp electrode for optimal wearing comfort," *Clinical Neurophysiology*, vol. 121, no. 7, pp. 1007–1014, 2010.

[2] S. D. Vann, J. P. Aggleton, and E. A. Maguire, "What does the retrosplenial cortex do?," *Nature Reviews Neuroscience*, vol. 10, no. 11, p. 792, 2009.

[3] B. A. Vogt, D. M. Finch, and C. R. Olson, "Functional heterogeneity in cingulate cortex: the anterior executive and posterior evaluative regions," *Cerebral cortex*, vol. 2, no. 6, pp. 435–443, 1992.

[4] G. Waterstraat, T. Fedele, M. Burghoff, H.-J. Scheer, and G. Curio, "Recording human cortical population spikes non-invasively–an eeg tutorial," *Journal of neuroscience methods*, vol. 250, pp. 74–84, 2015.

[5] G. Waterstraat, M. Scheuermann, and G. Curio, "Non-invasive single-trial detection of variable population spike responses in human somatosensory evoked potentials," *Clinical Neurophysiology*, vol. 127, no. 3, pp. 1872–1878, 2016.

[6] L. Iemi, M. Chaumon, S. M. Crouzet, and N. A. Busch, "Spontaneous neural oscillations bias perception by modulating baseline excitability," *Journal of Neuroscience*, vol. 37, no. 4, pp. 807–819, 2017.

[7] G. Waterstraat, G. Curio, and V. Nikulin, "On optimal spatial filtering for the detection of phase coupling in multivariate neural recordings," *NeuroImage*, 2017.

[8] R. S. Fisher, W. v. E. Boas, W. Blume, C. Elger, P. Genton, P. Lee, and J. Engel, "Epileptic seizures and epilepsy: definitions proposed by the international league against epilepsy (ilae) and the international bureau for epilepsy (ibe)," *Epilepsia*, vol. 46, no. 4, pp. 470–472, 2005.

[9] R. A. Brown, M. L. Lauzon, and R. Frayne, "A general description of linear time-frequency transforms and formulation of a fast, invertible transform that samples the continuous s-transform spectrum nonredundantly," *IEEE Transactions on Signal Processing*, vol. 58, no. 1, pp. 281–290, 2010.

[10] M. Tudor, L. Tudor, and K. I. Tudor, "Hans berger (1873-1941)–the history of electroencephalography," *Acta medica Croatica: casopis Hravatske akademije medicinskih znanosti*, vol. 59, no. 4, pp. 307–313, 2005.

[11] E. D. Adrian, "The impulses produced by sensory nerve endings," *The Journal of physiology*, vol. 61, no. 1, pp. 49–72, 1926.

[12] P. Brenni, R. Galdi, F. Pietra, and A. Savini, "From volta onwards: A variety of electrical batteries in the pavia museum of electrical technology," in *HISTory of ELectro-technology CONference (HISTELCON), 2012 Third IEEE*, pp. 1–6, IEEE, 2012.

[13] S. Finger, *Origins of neuroscience: a history of explorations into brain function*. Oxford University Press, USA, 2001.

[14] T. F. Collura, "History and evolution of electroencephalographic instruments and techniques.," *Journal of clinical neurophysiology*, vol. 10, no. 4, pp. 476–504, 1993.

[15] P. Tallgren, S. Vanhatalo, K. Kaila, and J. Voipio, "Evaluation of commercially available electrodes and gels for recording of slow eeg potentials," *Clinical Neurophysiology*, vol. 116, no. 4, pp. 799–806, 2005.

[16] A. Puce and M. S. Hämäläinen, "A review of issues related to data acquisition and analysis in eeg/meg studies," *Brain Sciences*, vol. 7, no. 6, p. 58, 2017.

[17] P. Fiedler, J. Haueisen, D. Jannek, S. Griebel, L. Zentner, F. Vaz, and C. Fonseca, "Comparison of three types of dry electrodes for electroencephalography," *Acta Imeko*, vol. 3, no. 3, pp. 33–37, 2014.

[18] A. Searle and L. Kirkup, "A direct comparison of wet, dry and insulating bioelectric recording electrodes," *Physiological measurement*, vol. 21, no. 2, p. 271, 2000.

[19] E. Trinka, H. Cock, D. Hesdorffer, A. O. Rossetti, I. E. Scheffer, S. Shinnar, S. Shorvon, and D. H. Lowenstein, "A definition and classification of status epilepticus–report of the ilae task force on classification of status epilepticus," *Epilepsia*, vol. 56, no. 10, pp. 1515–1523, 2015.

[20] R. S. Fisher, J. H. Cross, C. D'Souza, J. A. French, S. R. Haut, N. Higurashi, E. Hirsch, F. E. Jansen, L. Lagae, S. L. Moshé, *et al.*, "Instruction manual for the ilae 2017 operational classification of seizure types," *Epilepsia*, vol. 58, no. 4, pp. 531–542, 2017.

[21] A. M. Dale and M. I. Sereno, "Improved localizadon of cortical activity by combining eeg and meg with mri cortical surface reconstruction: a linear approach," *Journal of cognitive neuroscience*, vol. 5, no. 2, pp. 162–176, 1993.

[22] R. I. Goldman, J. M. Stern, J. Engel, and M. S. Cohen, "Acquiring simultaneous eeg and functional mri," *Clinical Neurophysiology*, vol. 111, no. 11, pp. 1974–1980, 2000.

[23] V. Menon and S. Crottaz-Herbette, "Combined eeg and fmri studies of human brain function," *Int Rev Neurobiol*, vol. 66, pp. 291–321, 2005.

[24] M. Seeck, F. Lazeyras, C. M. Michel, O. Blanke, C. Gericke, J. Ives, J. Delavelle, X. Golay, C.-A. Haenggeli, N. De Tribolet, *et al.*, "Non-invasive epileptic focus localization using eeg-triggered functional mri and electromagnetic tomography," *Electroencephalography and clinical Neurophysiology*, vol. 106, no. 6, pp. 508–512, 1998.

[25] M. Sommer, J. Meinhardt, H.-P. Volz, *et al.*, "Combined measurement of event-related potentials (erps) and fmri," *Acta neurobiologiae experimentalis*, vol. 63, no. 1, pp. 49–54, 2002.

[26] G. Waterstraat, B. Telenczuk, M. Burghoff, T. Fedele, H. J. Scheer, and G. Curio, "Are high-frequency (600Hz) oscillations in human somatosensory evoked potentials due to phase-resetting phenomena?," *Clinical Neurophysiology*, vol. 123, no. 10, pp. 2064–2073, 2012.

[27] D. B. Larremore, W. L. Shew, E. Ott, and J. G. Restrepo, "Effects of network topology, transmission delays, and refractoriness on the response of coupled excitable systems to a stochastic stimulus," *Chaos: An Interdisciplinary Journal of Nonlinear Science*, vol. 21, no. 2, p. 025117, 2011.

[28] D. B. Larremore, W. L. Shew, and J. G. Restrepo, "Predicting criticality and dynamic range in complex networks: effects of topology," *Physical review letters*, vol. 106, no. 5, p. 058101, 2011.

[29] W. L. Shew and D. Plenz, "The functional benefits of criticality in the cortex.," *The Neuroscientist : a review journal bringing neurobiology, neurology and psychiatry*, vol. 19, no. 1, pp. 88–100, 2013.

[30] G. Waterstraat, M. Burghoff, T. Fedele, V. Nikulin, H. J. Scheer, and G. Curio, "Non-invasive single-trial EEG detection of evoked human neocortical population spikes," *NeuroImage*, vol. 105, pp. 13–20, 2015.

[31] G. Waterstraat, T. Fedele, M. Burghoff, H. J. Scheer, and G. Curio, "Recording human cortical population spikes non-invasively–An EEG tutorial," *Journal of neuroscience methods*, vol. 250, pp. 74–84, 2015.

[32] S. Dähne, V. V. Nikulin, D. Ramírez, P. J. Schreier, K. R. Müller, and S. Haufe, "Finding brain oscillations with power dependencies in neuroimaging data," *NeuroImage*, vol. 96, pp. 334–348, 2014.

[33] F. S. Bao, X. Liu, and C. Zhang, "PyEEG: An open source python module for EEG/MEG feature extraction," *Computational Intelligence and Neuroscience*, vol. 2011, 2011.

[34] X. Wan, K. Iwata, J. Riera, M. Kitamura, and R. Kawashima, "Artifact reduction for simultaneous EEG/fMRI recording: Adaptive FIR reduction of imaging artifacts," *Clinical Neurophysiology*, vol. 117, no. 3, pp. 681–692, 2006.

[35] T. Ball, M. Kern, I. Mutschler, A. Aertsen, and A. Schulze-Bonhage, "Signal quality of simultaneously recorded invasive and non-invasive EEG," *NeuroImage*, vol. 46, no. 3, pp. 708–716, 2009.

[36] L. F. Heffer and J. B. Fallon, "A novel stimulus artifact removal technique for high-rate electrical stimulation," *Journal of Neuroscience Methods*, vol. 170, no. 2, pp. 277–284, 2008.

[37] R. Hardstone, S. S. Poil, G. Schiavone, R. Jansen, V. V. Nikulin, H. D. Mansvelder, and K. Linkenkaer-Hansen, "Detrended fluctuation analysis: A scale-free view on neuronal oscillations," *Frontiers in Physiology*, vol. 3 NOV, no. November, pp. 1–13, 2012.

[38] K. Linkenkaer-hansenVadim, "Long-Range Temporal Correlations and Scaling Behavior in Human Brain Oscillations," vol. 21, no. 4, pp. 1370–1377, 2011.

[39] M. Siegel, T. H. Donner, and A. K. Engel, "Spectral fingerprints of large-scale neuronal interactions," *Nature Reviews Neuroscience*, vol. 13, no. February, pp. 20–25, 2012.

[40] V. V. Nikulin, E. G. Jönsson, and T. Brismar, "Attenuation of long-range temporal correlations in the amplitude dynamics of alpha and beta neuronal oscillations in patients with schizophrenia," *NeuroImage*, vol. 61, no. 1, pp. 162–169, 2012.

[41] G. Nolte, O. Bai, L. Wheaton, Z. Mari, S. Vorbach, and M. Hallett, "Identifying true brain interaction from EEG data using the imaginary part of coherency," *Clinical Neurophysiology*, vol. 115, no. 10, pp. 2292–2307, 2004.

[42] K. Yu, K. Shen, S. Shao, W. C. Ng, and X. Li, "Bilinear common spatial pattern for single-trial ERP-based rapid serial visual presentation triage," *Journal of Neural Engineering*, vol. 9, no. 4, p. 046013, 2012.

[43] T. Ergenoglu, T. Demiralp, Z. Bayraktaroglu, M. Ergen, H. Beydagi, and Y. Uresin, "Alpha rhythm of the eeg modulates visual detection performance in humans," *Cognitive Brain Research*, vol. 20, no. 3, pp. 376–383, 2004.

[44] C. Babiloni, F. Vecchio, A. Bultrini, G. Luca Romani, and P. M. Rossini, "Pre-and poststimulus alpha rhythms are related to conscious visual perception: a high-resolution eeg study," *Cerebral cortex*, vol. 16, no. 12, pp. 1690–1700, 2005.

[45] N. A. Busch, J. Dubois, and R. VanRullen, "The phase of ongoing eeg oscillations predicts visual perception," *Journal of Neuroscience*, vol. 29, no. 24, pp. 7869–7876, 2009.

[46] B. C. Bays, K. M. Visscher, C. C. Le Dantec, and A. R. Seitz, "Alpha-band eeg activity in perceptual learning," *Journal of vision*, vol. 15, no. 10, pp. 7–7, 2015.

[47] E. A. Krupinski, "The importance of perception research in medical imaging," *Radiation medicine*, vol. 18, no. 6, pp. 329–334, 2000.

[48] J. S. P. Macdonald, S. Mathan, and N. Yeung, "Trial-by-trial variations in subjective attentional state are reflected in ongoing prestimulus eeg alpha oscillations," *Frontiers in psychology*, vol. 2, p. 82, 2011.

[49] P. Fries, "A mechanism for cognitive dynamics: neuronal communication through neuronal coherence," *Trends in cognitive sciences*, vol. 9, no. 10, pp. 474–480, 2005.

[50] W. Rall, "Electrophysiology of a dendritic neuron model," *Biophysical journal*, vol. 2, no. 2, pp. 145–167, 1962.

[51] D. McLelland and O. Paulsen, "Neuronal oscillations and the rate-to-phase transform: mechanism, model and mutual information," *The Journal of physiology*, vol. 587, no. 4, pp. 769–785, 2009.

[52] K. Gurney, T. J. Prescott, and P. Redgrave, "A computational model of action selection in the basal ganglia. i. a new functional anatomy," *Biological cybernetics*, vol. 84, no. 6, pp. 401–410, 2001.

[53] J. C. Houk, J. L. Davis, and D. G. Beiser, *Models of information processing in the basal ganglia*. MIT press, 1995.

[54] N. Kopell, G. Ermentrout, M. Whittington, and R. Traub, "Gamma rhythms and beta rhythms have different synchronization properties," *Proceedings of the National Academy of Sciences*, vol. 97, no. 4, pp. 1867–1872, 2000.

[55] G. Buzsaki, *Rhythms of the Brain*. Oxford University Press, 2006.

[56] M. A. B. Brazier, H. Petsche, *et al.*, "Synchronization of eeg activity in epilepsies," 1972.

[57] J. Weule *et al.*, "Detection of n: m phase locking from noisy data: application to magnetoencephalography," *Phys. Rev. Lett*, vol. 81, no. 15, pp. 3291–3294, 1998.

[58] M. G. Rosenblum, A. S. Pikovsky, and J. Kurths, "Phase synchronization of chaotic oscillators," *Physical review letters*, vol. 76, no. 11, p. 1804, 1996.

[59] S. Baillet and L. Garnero, "A bayesian approach to introducing anatomo-functional priors in the eeg/meg inverse problem," *IEEE transactions on Biomedical Engineering*, vol. 44, no. 5, pp. 374–385, 1997.

[60] R. D. Pascual-Marqui, "Review of methods for solving the eeg inverse problem," *International journal of bioelectromagnetism*, vol. 1, no. 1, pp. 75–86, 1999.

[61] C. H. Wolters, L. Grasedyck, and W. Hackbusch, "Efficient computation of lead field bases and influence matrix for the fem-based eeg and meg inverse problem," *Inverse problems*, vol. 20, no. 4, p. 1099, 2004.

[62] F. Mormann, K. Lehnertz, P. David, and C. E. Elger, "Mean phase coherence as a measure for phase synchronization and its application to the eeg of epilepsy patients," *Physica D: Nonlinear Phenomena*, vol. 144, no. 3, pp. 358–369, 2000.

[63] B. Schack, N. Vath, H. Petsche, H.-G. Geissler, and E. Möller, "Phase-coupling of theta–gamma eeg rhythms during short-term memory processing," *International Journal of Psychophysiology*, vol. 44, no. 2, pp. 143–163, 2002.

[64] B. J. Fisch, *Epilepsy and intensive care monitoring: principles and practice*. Demos Medical Publishing, 2009.

[65] A. Pourahmad and A. Mahnam, "Evaluation of a low-cost and low-noise active dry electrode for long-term biopotential recording," *Journal of medical signals and sensors*, vol. 6, no. 4, p. 197, 2016.

[66] A. B. Usakli, "Improvement of eeg signal acquisition: An electrical aspect for state of the art of front end," *Computational intelligence and neuroscience*, vol. 2010, p. 12, 2010.

[67] G. O'Grady, N. Paskaranandavadivel, T. Angeli, P. Du, J. Windsor, L. Cheng, and A. Pullan, "A comparison of gold versus silver electrode contacts for high-resolution gastric electrical mapping using flexible printed circuit board arrays," *Physiological measurement*, vol. 32, no. 3, p. N13, 2011.

[68] P. Denes and R. Naunton, "Masking in pure-tone audiometry," 1952.

[69] P. Welch, "The use of fast fourier transform for the estimation of power spectra: a method based on time averaging over short, modified periodograms," *IEEE Transactions on audio and electroacoustics*, vol. 15, no. 2, pp. 70–73, 1967.

[70] T. Fedele, H. Scheer, M. Burghoff, G. Waterstraat, V. Nikulin, and G. Curio, "Distinction between added-energy and phase-resetting mechanisms in non-invasively detected somatosensory evoked responses," in *Engineering in medicine and biology society (EMBC), 2013 35th annual international conference of the IEEE*, pp. 1688–1691, IEEE, 2013.

[71] H. Scheer, T. Fedele, G. Curio, and M. Burghoff, "Extension of non-invasive eeg into the khz range for evoked thalamocortical activity by means of very low noise amplifiers," *Physiological measurement*, vol. 32, no. 12, p. N73, 2011.

[72] R. Hardstone, S.-S. Poil, G. Schiavone, R. Jansen, V. V. Nikulin, H. D. Mansvelder, and K. Linkenkaer-Hansen, "Detrended fluctuation analysis: a scale-free view on neuronal oscillations," *Frontiers in physiology*, vol. 3, 2012.

[73] B. B. Mandelbrot, *The fractal geometry of nature*, vol. 1. WH freeman New York, 1982.

[74] N. Schaworonkow, D. A. Blythe, J. Kegeles, G. Curio, and V. V. Nikulin, "Power-law dynamics in neuronal and behavioral data introduce spurious correlations," *Human brain mapping*, vol. 36, no. 8, pp. 2901–2914, 2015.

[75] A. Papoulis, *Signal analysis*, vol. 191. McGraw-Hill New York, 1977.

[76] M. HÃmÃlÃinen, "Mne software userâs guide version 2.7," 2009.

[77] A. M. Dale, A. K. Liu, B. R. Fischl, R. L. Buckner, J. W. Belliveau, J. D. Lewine, and E. Halgren, "Dynamic statistical parametric mapping: combining fmri and meg for high-resolution imaging of cortical activity," *Neuron*, vol. 26, no. 1, pp. 55–67, 2000.

[78] A. N. Tikhonov, "On the solution of ill-posed problems and the method of regularization," in *Doklady Akademii Nauk*, vol. 151, pp. 501–504, Russian Academy of Sciences, 1963.

[79] A. N. Tikhonov, A. Goncharsky, V. Stepanov, and A. G. Yagola, *Numerical methods for the solution of ill-posed problems*, vol. 328. Springer Science & Business Media, 2013.

[80] A. B. Tort, R. Komorowski, H. Eichenbaum, and N. Kopell, "Measuring phase-amplitude coupling between neuronal oscillations of different frequencies," *Journal of neurophysiology*, vol. 104, no. 2, pp. 1195–1210, 2010.

[81] S. Kullback and R. A. Leibler, "On information and sufficiency," *The annals of mathematical statistics*, vol. 22, no. 1, pp. 79–86, 1951.

[82] J. M. Joyce, "Kullback-leibler divergence," in *International Encyclopedia of Statistical Science*, pp. 720–722, Springer, 2011.

[83] R. T. Canolty, E. Edwards, S. S. Dalal, M. Soltani, S. S. Nagarajan, H. E. Kirsch, M. S. Berger, N. M. Barbaro, and R. T. Knight, "High gamma power is phase-locked to theta oscillations in human neocortex," *science*, vol. 313, no. 5793, pp. 1626–1628, 2006.

[84] G. Waterstraat, L. Iemi, I. de Almeida Ivo, G. Curio, and V. Nikulin, "P20. disentangling the effect of pre-stimulus oscillatory power on visual detection using spatio-spectral decomposition and heterogeneous choice models," *Clinical Neurophysiology*, vol. 129, no. 8, p. e75, 2018.

Appendix

Epilepsy Patient Trial

The patient gave his verbal consent for some test run trials but due to a couple of reasons follow through with a consistent experiment was not reached. The trial of this subject was recorded but unanalised since its preparation lacked method.

This experiment was conducted early on, before the plasticised cables were included as part of the manufacturing, which led to some technical issues: upon the application of the system on the subject's scalp many electrodes broke, the application by itself proved to be a lengthy process since the cables were so difficult to distinguish and tangled up during the process. Additionally, regarding recyclability, all but one electrode broke upon removal of the setup.

For the specific time period, unfortunately for this experiment but fortunately and as a result of medication, the patient did not demonstrate many epileptic episodes. Two specific moments were regarded by the medical staff as being epileptic seizures, but those were not recorded as the setup was still in process.

Further Results

Criticality in High Frequency Oscillations

Figure 6.1: Detrended Fluctuation Analysis for subject K001

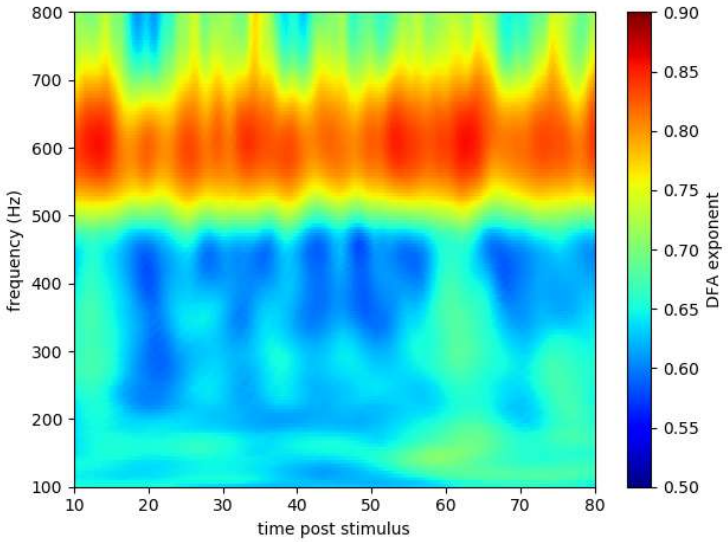

Figure 6.2: Optimal fit for the LSD for subject K001

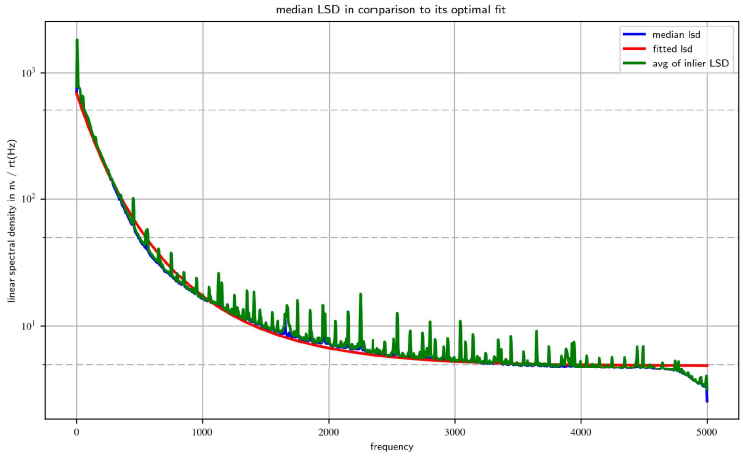

Figure 6.3: Time Frequency Analysis without noise for subject K001

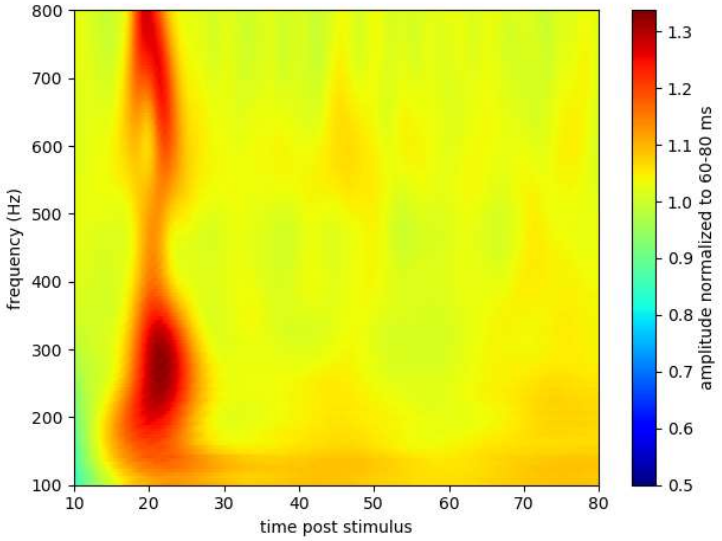

Figure 6.4: Patterns of the significant burst for subject K001

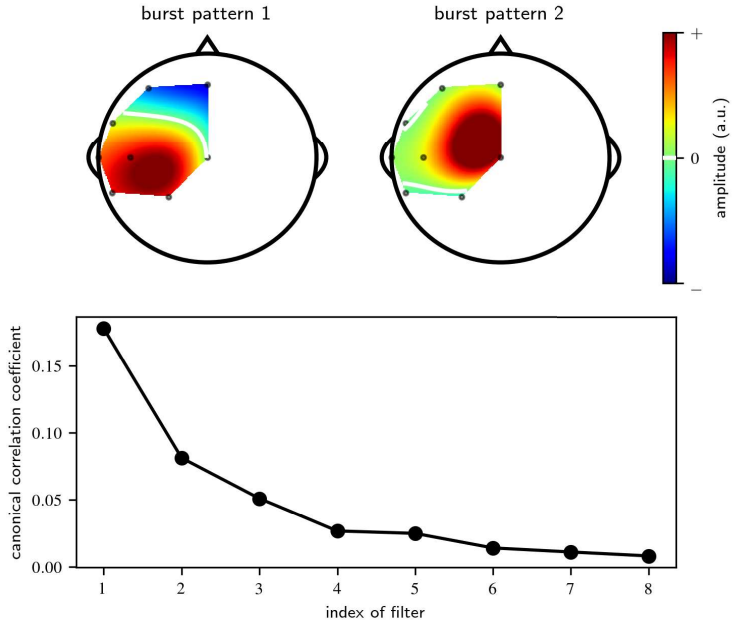

Figure 6.5: Detrended Fluctuation Analysis for subject K003

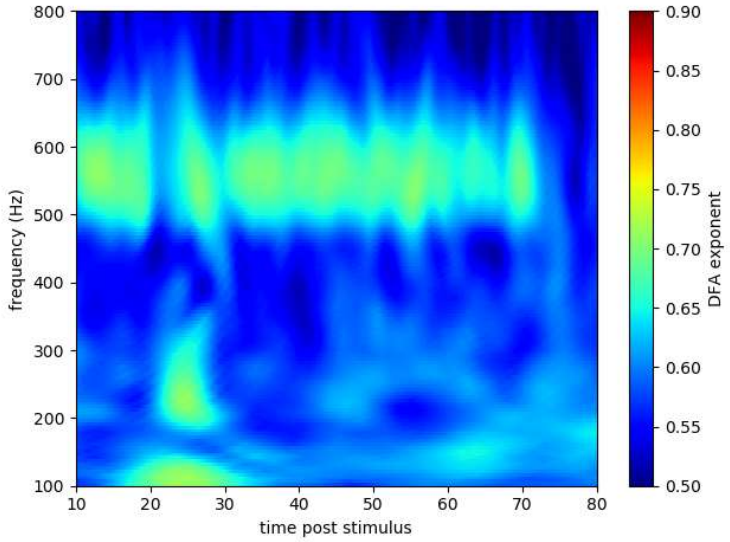

Figure 6.6: Optimal fit for the LSD for subject K003

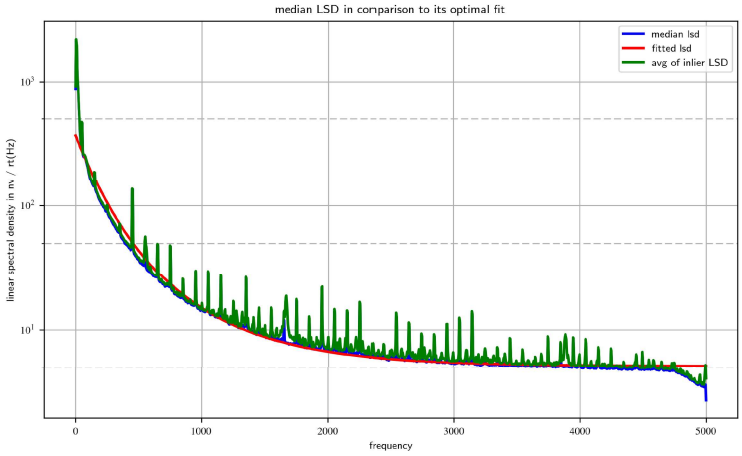

Figure 6.7: Time Frequency Analysis without noise for subject K003

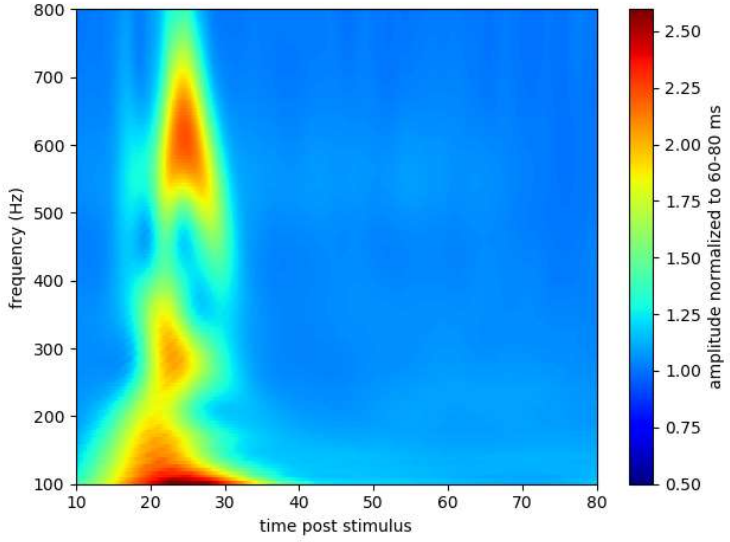

Figure 6.8: Patterns of the significant burst for subject K003

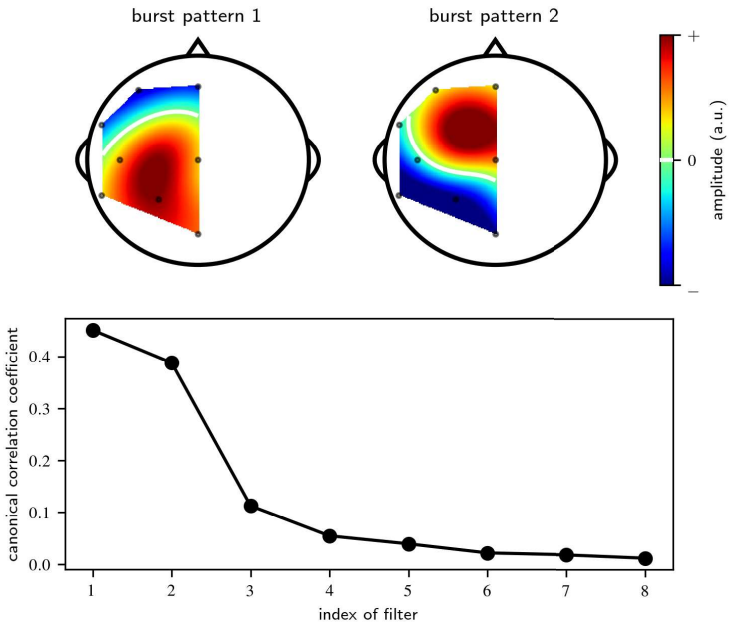

Figure 6.9: Detrended Fluctuation Analysis for subject K004

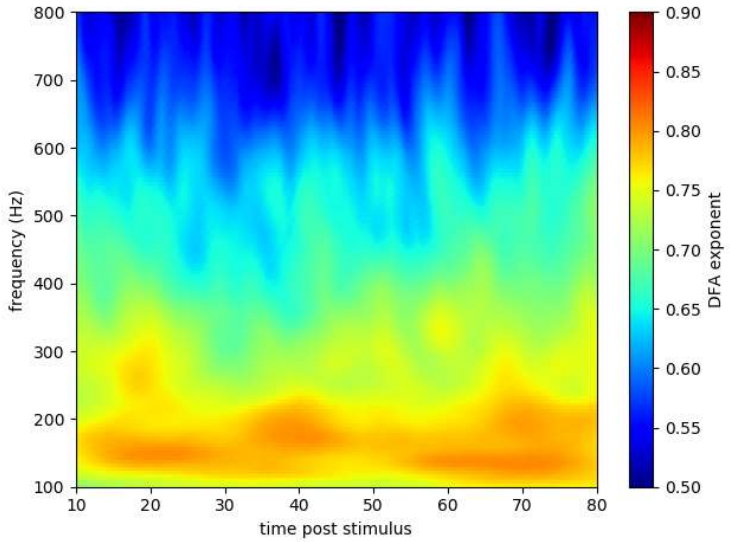

Figure 6.10: Optimal fit for the LSD for subject K004

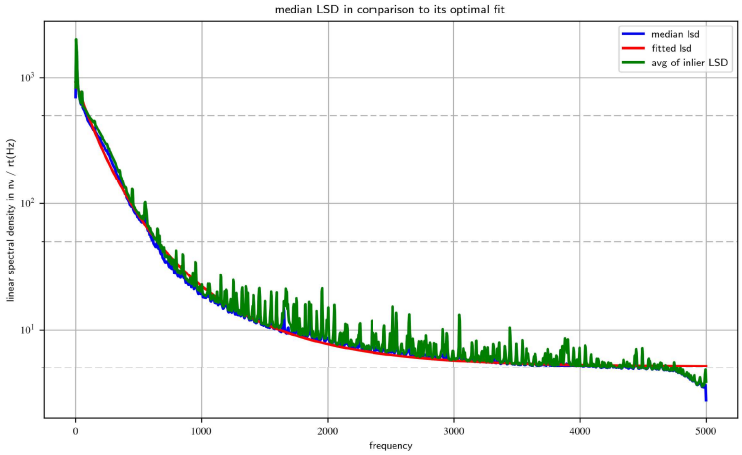

Figure 6.11: Time Frequency Analysis without noise for subject K004

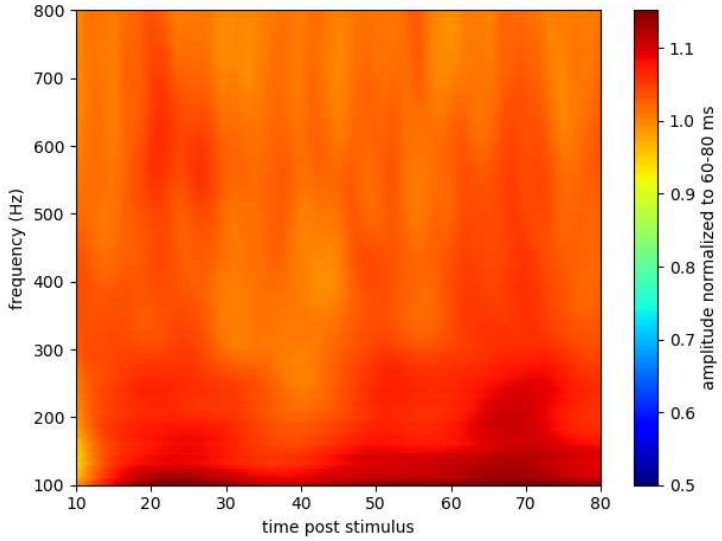

Figure 6.12: Patterns of the significant burst for subject K004

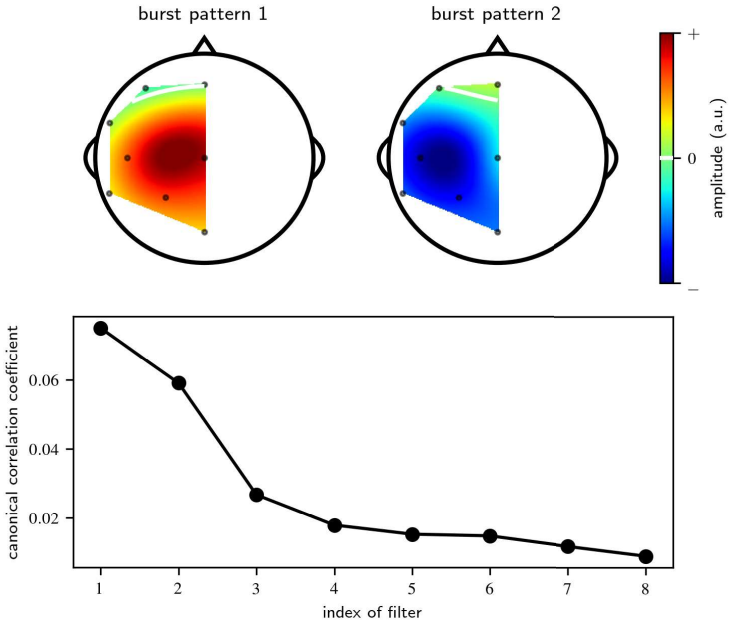

Figure 6.13: Detrended Fluctuation Analysis for subject K005

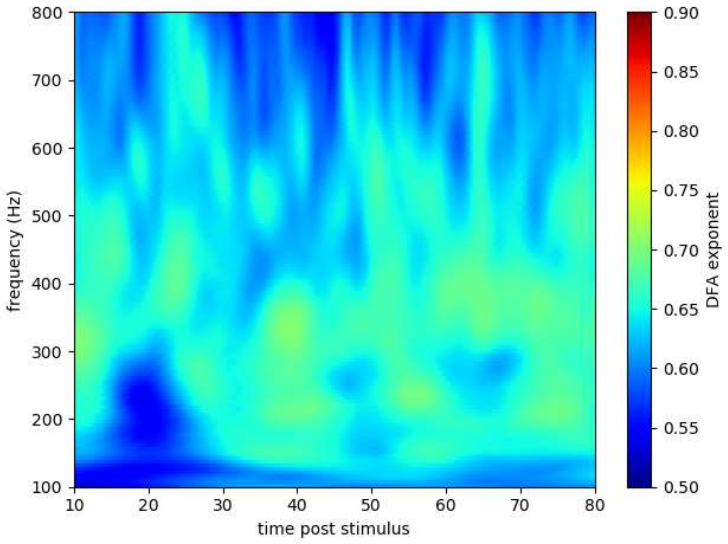

Figure 6.14: Optimal fit for the LSD for subject K005

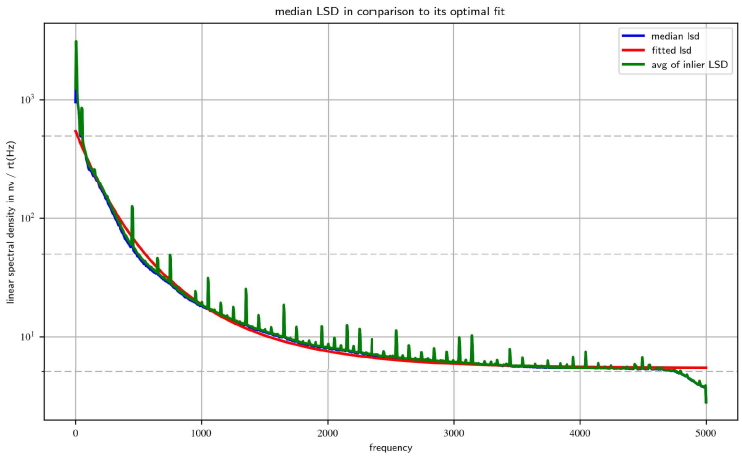

Figure 6.15: Time Frequency Analysis without noise for subject K005

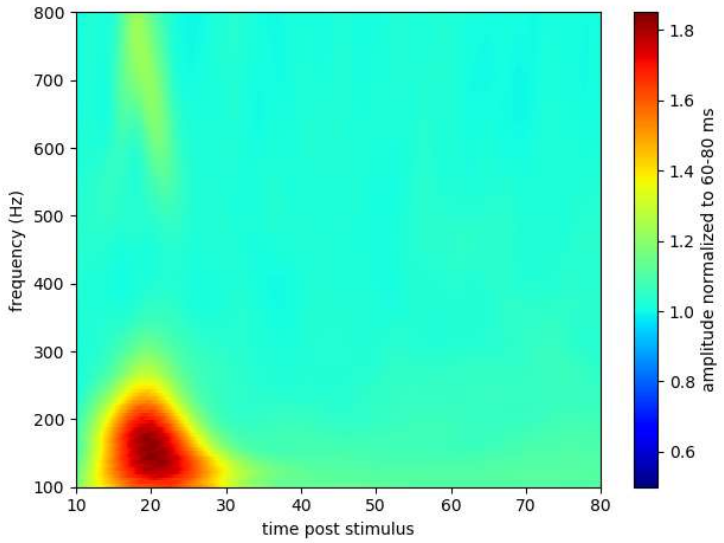

Figure 6.16: Patterns of the significant burst for subject K005

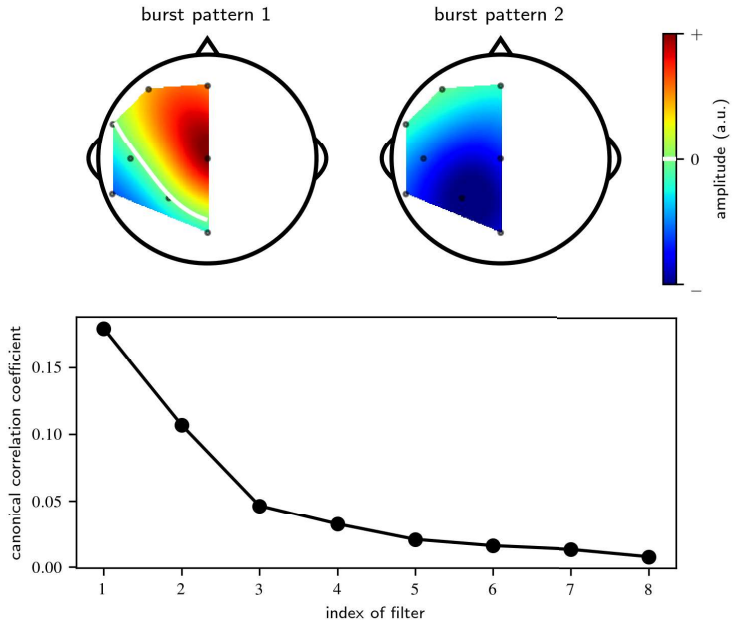

Figure 6.17: Detrended Fluctuation Analysis for subject K006

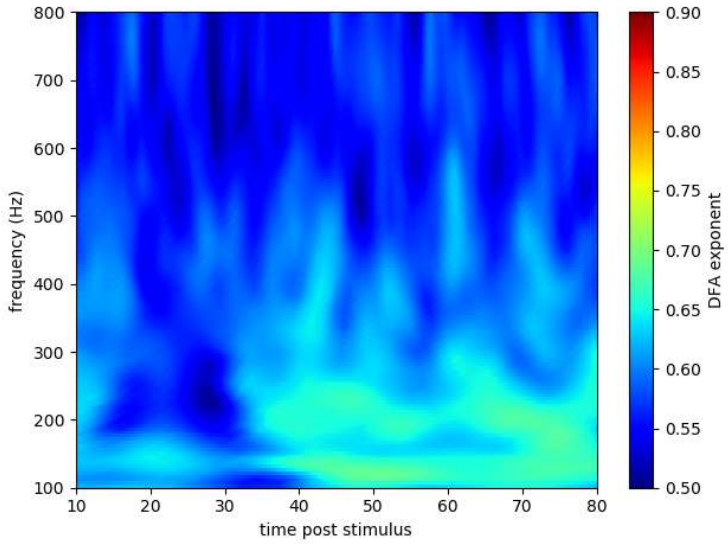

Figure 6.18: Optimal fit for the LSD for subject K006

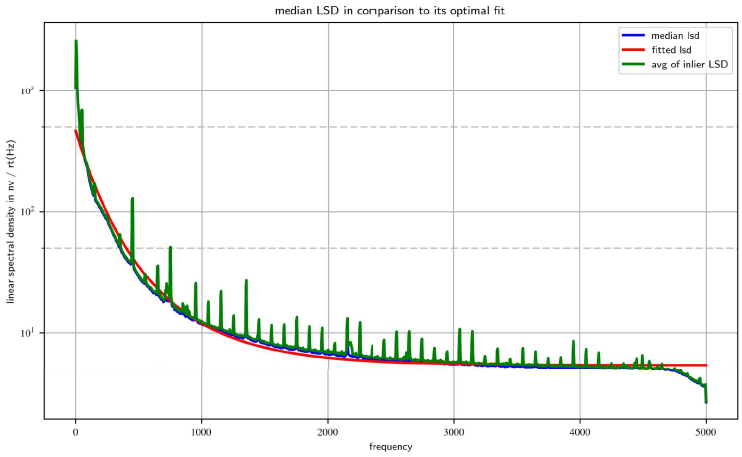

Figure 6.19: Time Frequency Analysis without noise for subject K006

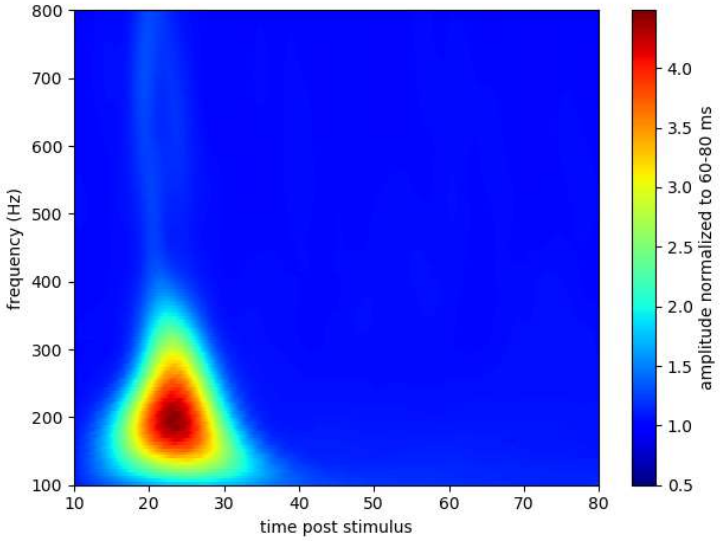

Figure 6.20: Patterns of the significant burst for subject K006

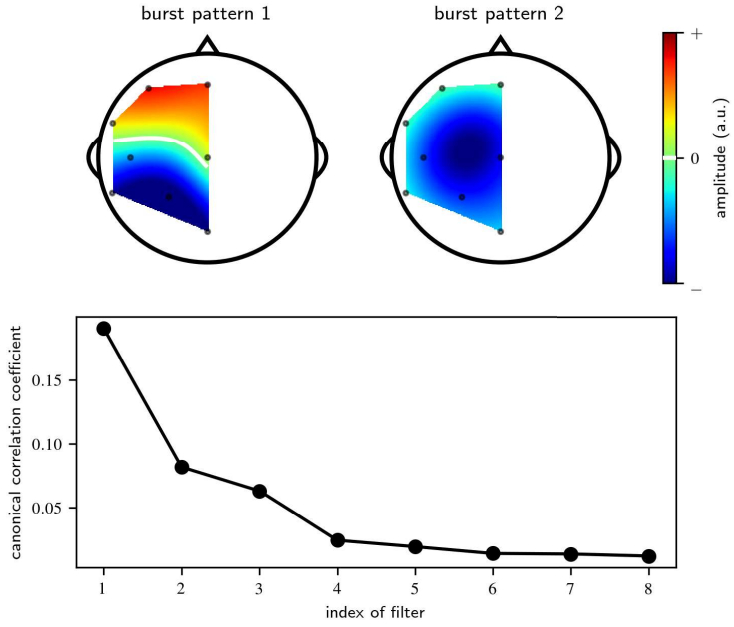

Figure 6.21: Detrended Fluctuation Analysis for subject K007

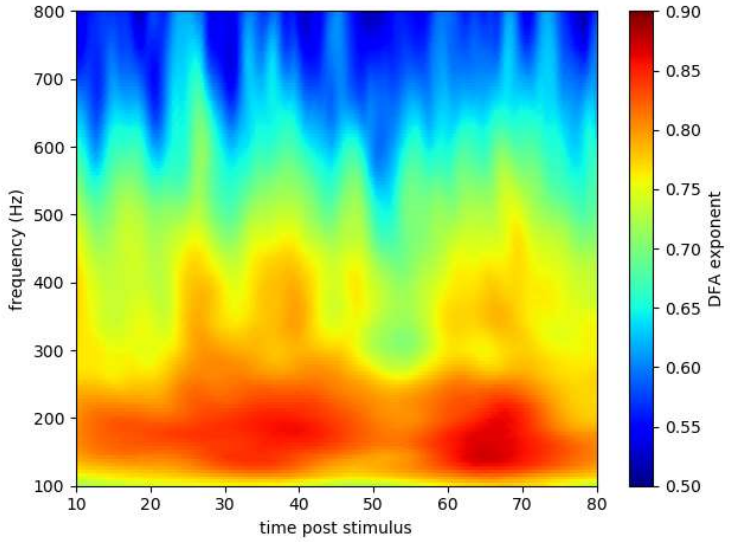

Figure 6.22: Optimal fit for the LSD for subject K007

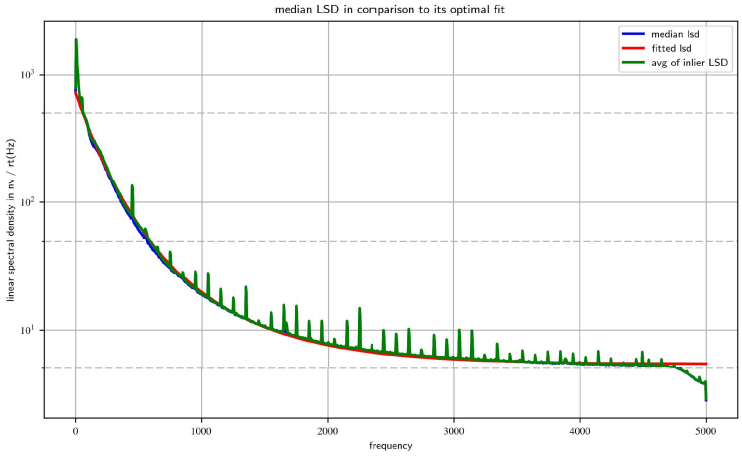

Figure 6.23: Time Frequency Analysis without noise for subject K007

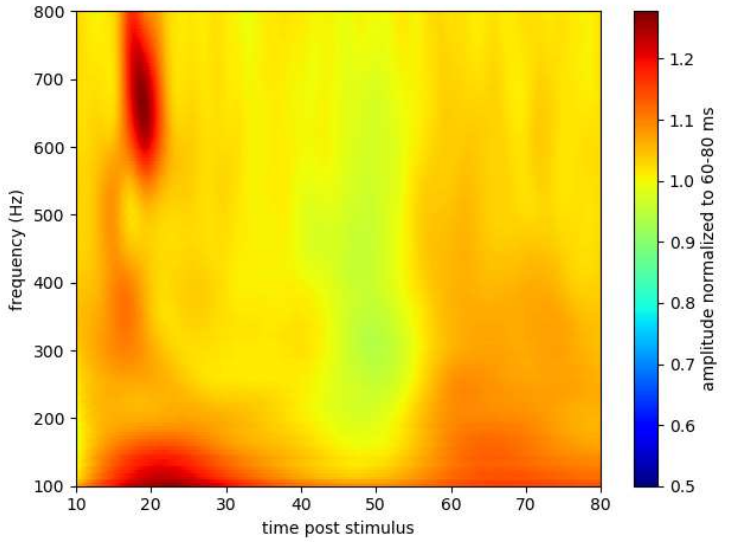

Figure 6.24: Patterns of the significant burst for subject K007

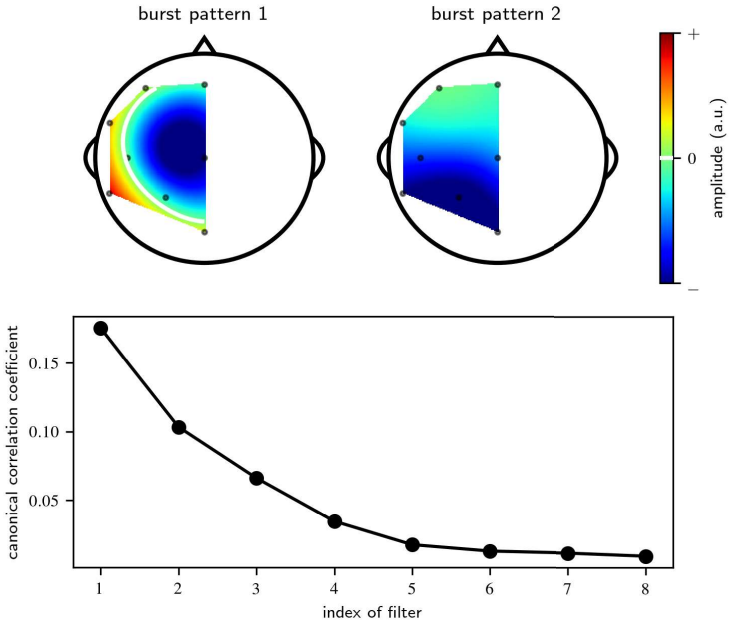

Figure 6.25: Detrended Fluctuation Analysis for subject K008

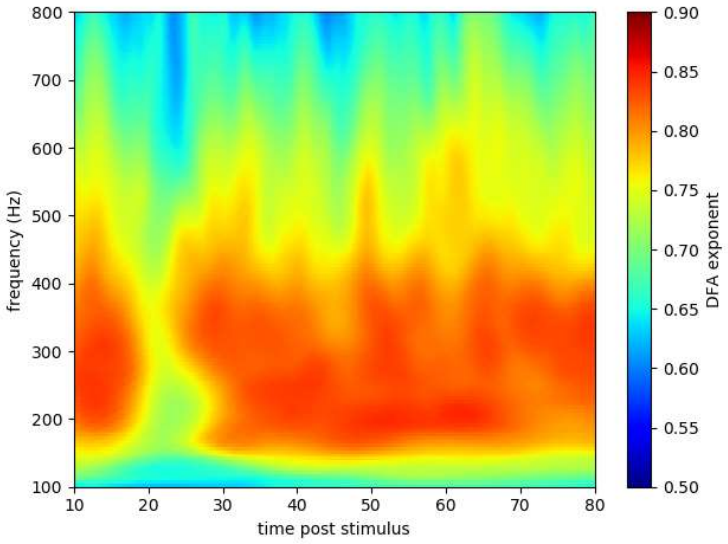

Figure 6.26: Optimal fit for the LSD for subject K008

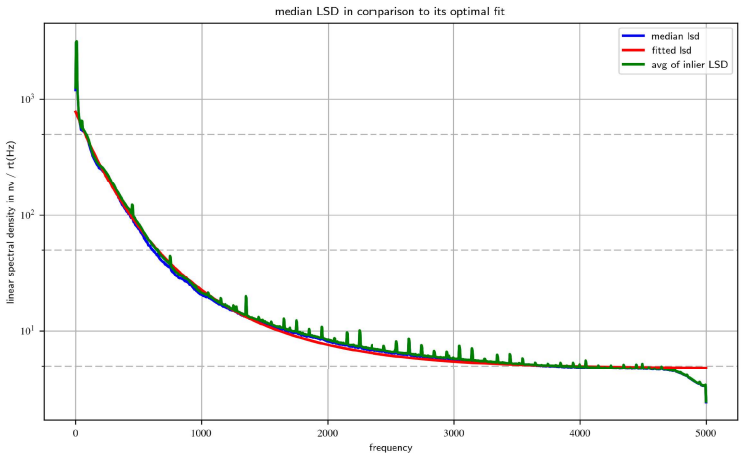

Figure 6.27: Time Frequency Analysis without noise for subject K008

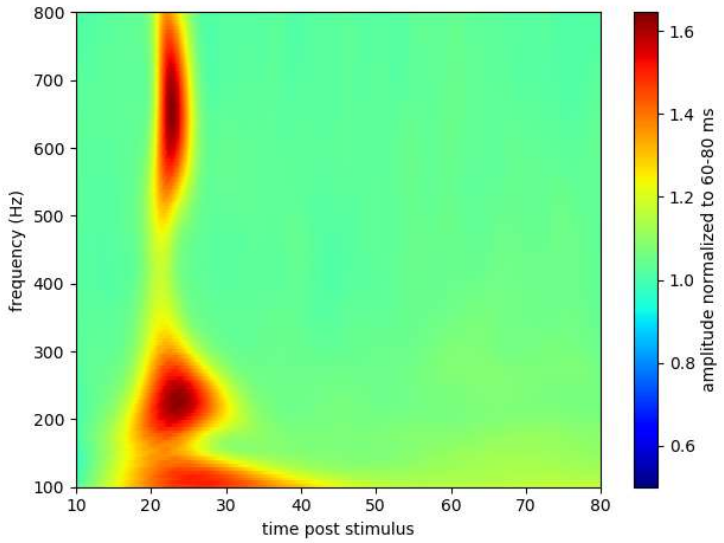

Figure 6.28: Patterns of the significant burst for subject K008

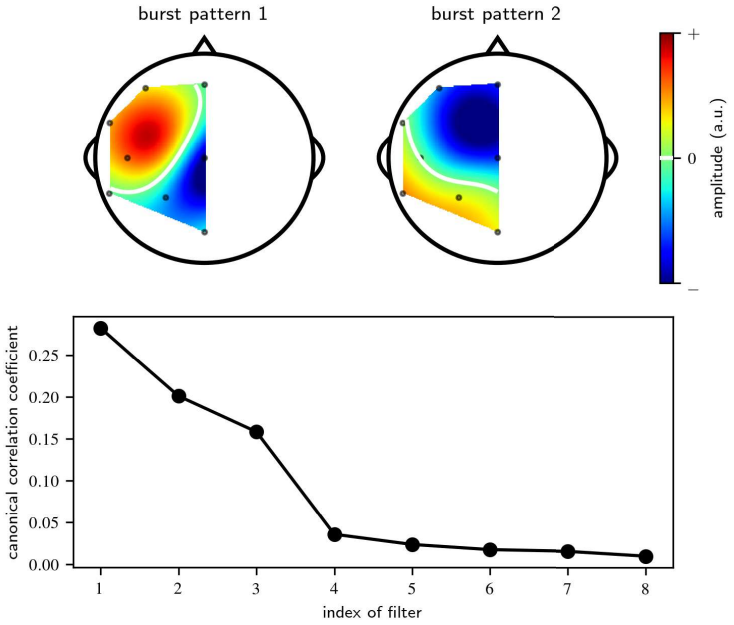

Figure 6.29: Detrended Fluctuation Analysis for subject K009

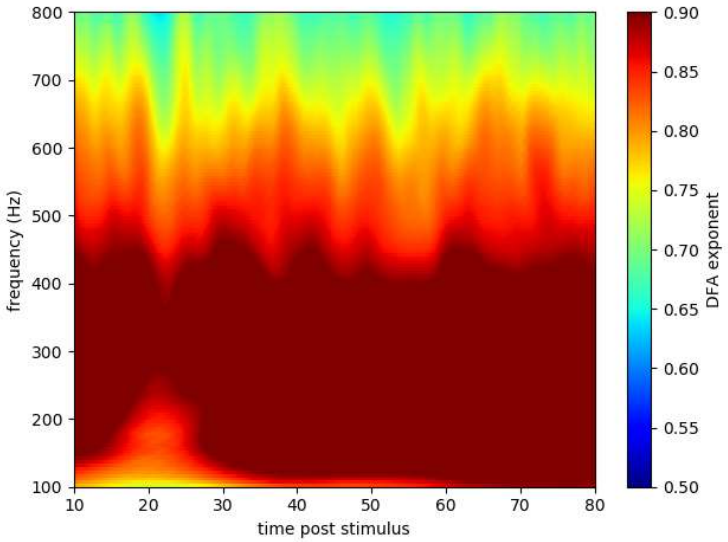

Figure 6.30: Optimal fit for the LSD for subject K009

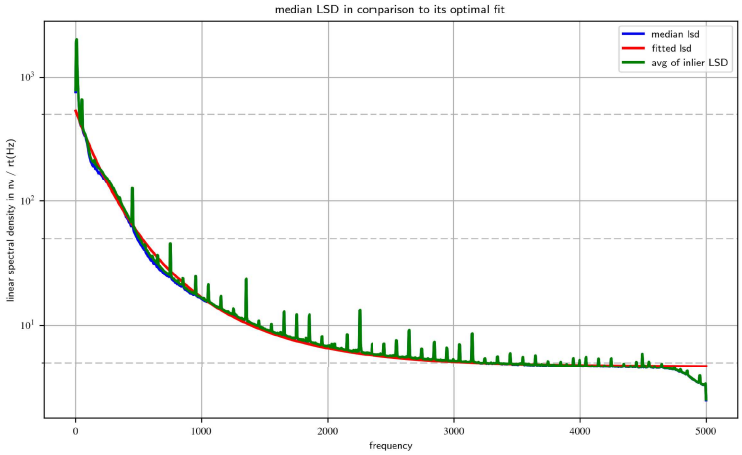

Figure 6.31: Time Frequency Analysis without noise for subject K009

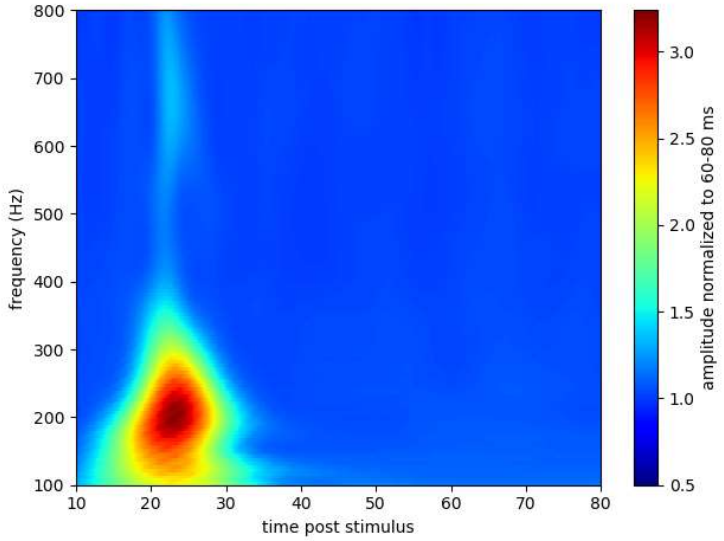

Figure 6.32: Patterns of the significant burst for subject K009

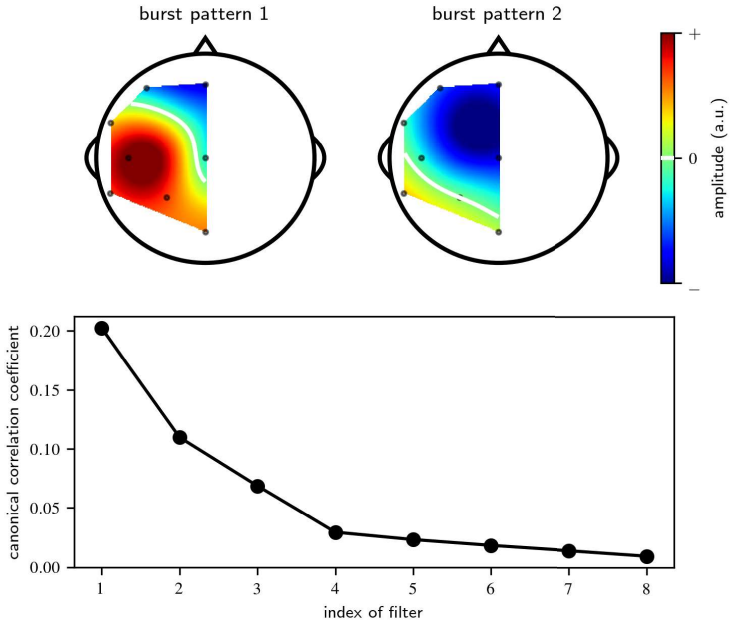

Figure 6.33: Detrended Fluctuation Analysis for subject K010

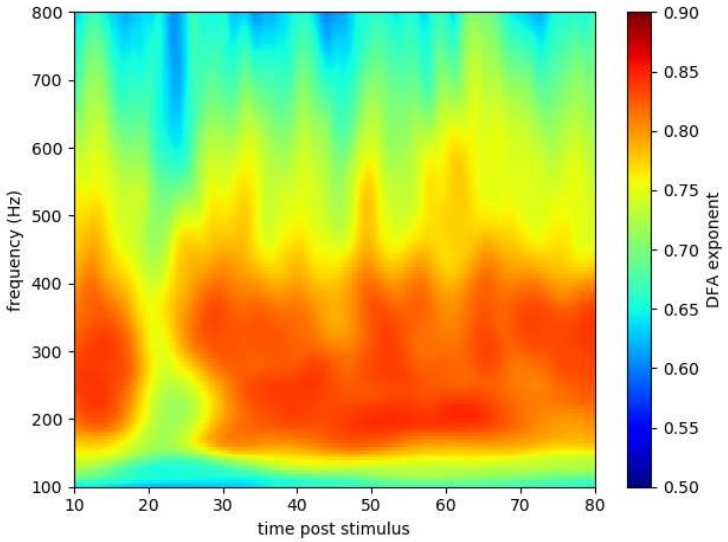

Figure 6.34: Optimal fit for the LSD for subject K010

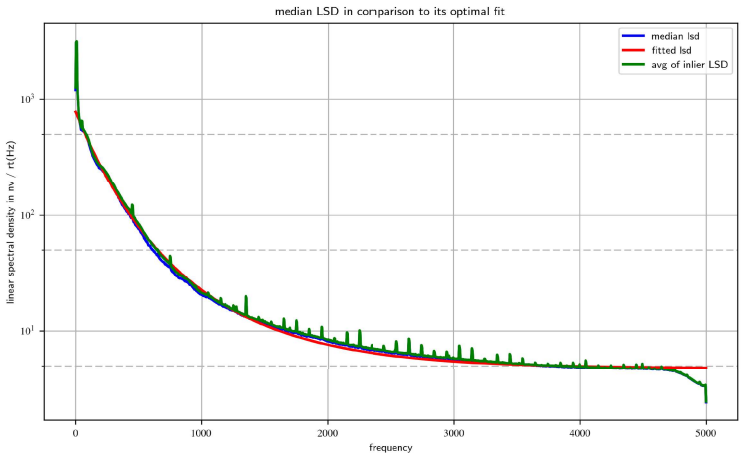

Figure 6.35: Time Frequency Analysis without noise for subject K010

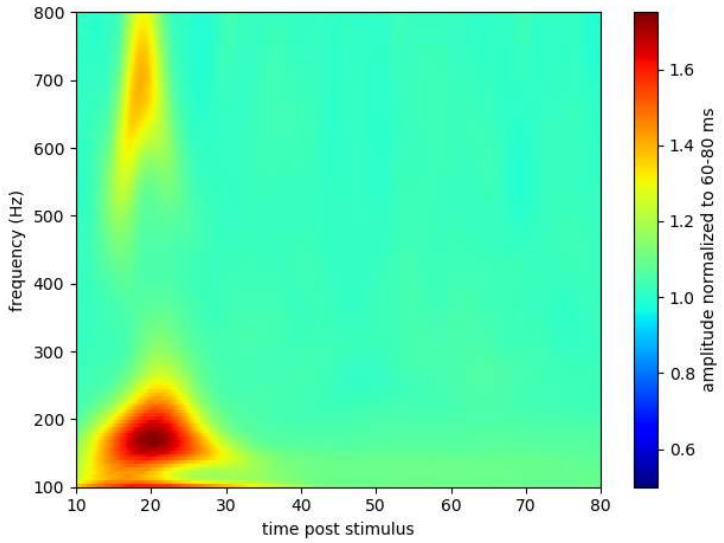

Figure 6.36: Patterns of the significant burst for subject K010